Mon. Not. R. Astron. Soc. **394,** 2266–2282 (2009) doi:10.1111/j.1365-2966.2009.14505.x

SN 2005cs in M51 – II. Complete evolution in the optical and the near-infrared

A. Pastorello,[1⋆] S. Valenti,[1] L. Zampieri,[2] H. Navasardyan,[2] S. Taubenberger,[3] S. J. Smartt,[1] A. A. Arkharov,[4] O. Bärnbantner,[5] H. Barwig,[5] S. Benetti,[2] P. Birtwhistle,[6] M. T. Botticella,[1] E. Cappellaro,[2] M. Del Principe,[7] F. Di Mille,[8] G. Di Rico,[7] M. Dolci,[7] N. Elias-Rosa,[9] N. V. Efimova,[4,10] M. Fiedler,[11] A. Harutyunyan,[2,12] P. A. Höflich,[13] W. Kloehr,[14] V. M. Larionov,[4,10,15] V. Lorenzi,[12] J. R. Maund,[16,17] N. Napoleone,[18] M. Ragni,[7] M. Richmond,[19] C. Ries,[5] S. Spiro,[1,18,20] S. Temporin,[21] M. Turatto[22] and J. C. Wheeler[17]

[1]*Astrophysics Research Centre, School of Mathematics and Physics, Queen's University Belfast, Belfast BT7 1NN*
[2]*INAF Osservatorio Astronomico di Padova, Vicolo dell'Osservatorio 5, 35122 Padova, Italy*
[3]*Max-Planck-Institut für Astrophysik, Karl-Schwarzschild-Str. 1, 85741 Garching bei München, Germany*
[4]*Central Astronomical Observatory of Pulkovo, 196140 St Petersburg, Russia*
[5]*Universitäts-Sternwarte München, Scheinerstr. 1, 81679 München, Germany*
[6]*Great Shefford Observatory, Phlox Cottage, Wantage Road, Great Shefford RG17 7DA*
[7]*INAF Osservatorio Astronomico di Collurania, via M. Maggini, 64100 Teramo, Italy*
[8]*Dipartmento of Astronomia, Universitá di Padova, Vicolo dell'Osservatorio 2, 35122 Padova, Italy*
[9]*Spitzer Science Center, California Institute of Technology, 1200 East California Blvd., Pasadena, CA 91125, USA*
[10]*Astronomical Institute of St Petersburg University, St Petersburg, Petrodvorets, Universitetsky pr. 28, 198504 St Petersburg, Russia*
[11]*Astroclub Radebeul, Auf den Ebenbergen 10a, 01445 Radebeul, Germany*
[12]*Fundación Galileo Galilei-INAF, Telescopio Nazionale Galileo, 38700 Santa Cruz de la Palma, Tenerife, Spain*
[13]*Department of Physics, Florida State University, 315 Keen Building, Tallahassee, FL 32306-4350, USA*
[14]*Gretelbaumbachstr. 31, 97424 Schweinfurt, Germany*
[15]*Isaac Newton Institute of Chile, St Petersburg Branch*
[16]*Dark Cosmology Centre, Niels Bohr Institute, University of Copenhagen, Juliane Maries Vej 30, 2100 Copenhagen, Denmark*
[17]*Department of Astronomy and McDonald Observatory, The University of Texas at Austin, 1 University Station, C1400 Austin, Texas 78712-0259, USA*
[18]*INAF Osservatorio Astronomico di Roma, Via di Frascati 33, 00040 Monte Porzio Catone, Italy*
[19]*Department of Physics, Rochester Institute of Technology, 85 Lomb Memorial Drive, Rochester, NY 14623-5603, USA*
[20]*Dipartimento di Fisica, Universitá di Roma Tor Vergata, Via della Ricerca Scientifica 1, 00133 Roma, Italy*
[21]*CEA Sacly, DSM/IRFU/SAp, AIM – Unité Mixte de Recherche CEA – CNRS – Université Paris Diderot – UMR715, 91191 Gif-sur-Yvette, France*
[22]*INAF Osservatorio Astrofisico di Catania, Via S. Sofia 78, 95123 Catania, Italy*

Accepted 2009 January 13. Received 2009 January 12; in original form 2008 December 8

ABSTRACT

We present the results of the one-year long observational campaign of the type II plateau SN 2005cs, which exploded in the nearby spiral galaxy M51 (the Whirlpool galaxy). This extensive data set makes SN 2005cs the best observed low-luminosity, ^{56}Ni-poor type II plateau event so far and one of the best core-collapse supernovae ever. The optical and near-infrared spectra show narrow P-Cygni lines characteristic of this SN family, which are indicative of a very low expansion velocity (about 1000 km s^{-1}) of the ejected material. The optical light curves cover both the plateau phase and the late-time radioactive tail, until about 380 d after core-collapse. Numerous unfiltered observations obtained by amateur astronomers give us the rare opportunity to monitor the fast rise to maximum light, lasting about 2 d. In addition to optical observations, we also present near-infrared light curves that (together with already published ultraviolet observations) allow us to construct for the first time a reliable bolometric light curve for an object of this class. Finally, comparing the observed data with

⋆E-mail: a.pastorello@qub.ac.uk

those derived from a semi-analytic model, we infer for SN 2005cs a ^{56}Ni mass of about $3 \times 10^{-3}\,M_{\odot}$, a total ejected mass of 8–13 $M_{\odot}$ and an explosion energy of about 3×10^{50} erg.

Key words: supernovae: general – supernovae: individual: SN 2005cs – supernovae: individual: SN 1997D – supernovae: individual: SN 1999br – supernovae: individual: SN 2003Z – galaxies: individual: M51.

1 INTRODUCTION

Underluminous, low-energy, ^{56}Ni-poor type IIP supernovae (SNe IIP) form one of the most debated core-collapse supernova (CC SN) subgroups due to the unveiled nature of their progenitors. The controversy started with the discovery of the puzzling SN 1997D (Turatto et al. 1998; Benetti et al. 2001). The unusual characteristics of this SN were well modelled with either a core-collapse explosion of a very massive (more than 20 $M_{\odot}$) star with large fallback of material (Zampieri, Shapiro & Colpi 1998), or with the explosion of a less massive progenitor (8–10 $M_{\odot}$; Chugai & Utrobin 2000), close in mass to the lower limit for stars which can undergo core-collapse.

Several other SNe have been found sharing observational properties with SN 1997D, viz. SNe 1994N, 1999br, 1999eu, 2001dc (Pastorello et al. 2004), while data for another group of low-luminosity SNe IIP (SNe 1999gn, 2002gd, 2003Z, 2004eg, 2006ov) will be presented by Spiro et al. (in preparation). SN 1999br, in particular, had even more extreme observed properties than SN 1997D (see also Hamuy 2003; Pastorello 2003). Despite the modelling of the light-curve and spectral evolution of SN 1999br suggested that the precursor was a 16 $M_{\odot}$ star (Zampieri et al. 2003), direct measurements based on a marginal detection on pre-explosion *Hubble Space Telescope* (*HST*) archival images (see van Dyk, Li & Filippenko 2003; Maund & Smartt 2005) indicated a progenitor with upper mass limit of 12 $M_{\odot}$. Smartt et al. (2008) recently revised this estimate, increasing the upper limit up to 15 $M_{\odot}$. However, we have to admit that, due to the uncertainties on dust extinction and to the lack of colour information, the mass limit for the progenitor of SN 1999br still remains poorly constrained.

In the context of faint transients, it is worth mentioning also the extreme case of a recent transient in M85. Although Ofek et al. (2007), Kulkarni et al. (2007) and Rau et al. (2007) classified it as an anomalous, luminous red nova possibly resulting from a rather exotic stellar merger, it shares some similarities with the SN 1997D-like events (resembling also a faint type IIn SN). As a consequence, it would be the faintest SN II ever discovered (Pastorello et al. 2007). Moreover, Valenti et al. (2009) present a study of the faintest SN Ib/c ever discovered, SN 2008ha, and propose that the whole family of objects similar to SN 2002cx and previously classified as peculiar type Ia SNe (e.g. Li et al. 2003) are instead underluminous, stripped-envelope core-collapse SNe.

The first opportunity to study fairly well the progenitor of an underluminous SN IIP and its environment was given by SN 2005cs. The short distance of the host galaxy (M51) allowed to univocally recover the precursor star in a set of *HST* images obtained before the SN explosion (Maund, Smartt & Danziger 2005; Li et al. 2006). The progenitor appeared to be a red supergiant (RSG) with an absolute V-band magnitude around -6 and initial mass of 7–13 $M_{\odot}$. This mass range is also in excellent agreement with that derived by Takáts & Vinkó (2006, about 9 $M_{\odot}$) using an updated host galaxy distance estimate, based on both the Expanding Photosphere Method (EPM) and the Standard Candles Method (SCM), and with the estimate obtained by Eldridge, Mattila & Smartt (2007, 6–8 $M_{\odot}$) studying the expected optical and near-infrared (NIR) magnitudes for RSG stars. The only attempt performed so far to determine the mass of the precursor of SN 2005cs via hydrodynamic modelling of the SN data (Utrobin & Chugai 2008) gave a remarkably higher pre-SN mass ($17.3 \pm 1.0\,M_{\odot}$).

In Pastorello et al. (2006) (hereafter Paper I) the evolution of SN 2005cs at optical wavelengths during the first month after explosion was shown. Early-time data were also presented by Li et al. (2006), Tsvetkov et al. (2006), Gnedin et al. (2007), Brown et al. (2007), Dessart et al. (2008). Data of Brown et al. (2007) are of particular importance because they show for the first time the early-time evolution of an underluminous SN IIP in the ultraviolet (UV) and X-ray domains.

The distance to M51 adopted in Paper I was $d = 8.4$ Mpc (based on planetary nebula luminosity function; Feldmeier, Ciardullo & Jacoby 1997). However, Takáts & Vinkó (2006), averaging their EPM- and SCM-based estimates with others available in literature, proposed a distance of 7.1 ± 1.2 Mpc, which is significantly lower than that of Feldmeier et al. (1997). Since most independent methods appear to converge to lower values for the distance, in this paper we will adopt the average estimate of Takáts & Vinkó (2006), which corresponds to distance modulus $\mu = 29.26 \pm 0.33$.

The total extinction in the direction of SN 2005cs is also quite debated, although there is clear evidence from spectroscopy that the SN light is only marginally reddened. In Paper I, a colour excess of $E(B - V) = 0.11$ mag was adopted. Maund et al. (2005) and Li et al. (2006) suggested even higher reddening values, i.e. $E(B - V) = 0.14$ and 0.12 mag, respectively. However, spectral models presented by Baron, Branch & Hauschildt (2007) reproduce well the observed spectra of SN 2005cs dereddened by a lower amount, about 0.035–0.050 mag (0.035 mag is the Galactic reddening reported by Schlegel, Finkbeiner & Davis 1998). We find the arguments presented by Baron et al. (2007) convincing, and adopt hereafter a reddening of $E(B - V) = 0.05$ mag.

In this paper we present the entire collection of optical and NIR data of SN 2005cs, obtained through a coordinated observational campaign which lasted for more than one year and was performed using a number of different telescopes. We also include in our analysis optical photometry presented in Paper I and preliminarily calibrated making use of the same sequence of stars used in the study of the type Ic SN 1994I (Richmond et al. 1996). Data from Paper I have been recalibrated using a new, wider sequence of local standards (labelled with numbers or capital letters, Fig. 1), whose magnitudes and errors are reported in Table 1.

The manuscript is organized as follows. In Section 2 we present the optical and NIR photometric data of SN 2005cs, in Section 3 we compute its bolometric light curve and compare it with those of other SNe IIP, while in Section 4 we analyse the entire spectral sequence. In Section 5 we discuss the nature of the progenitor of SN 2005cs, through the modelling of the observed data of the SN

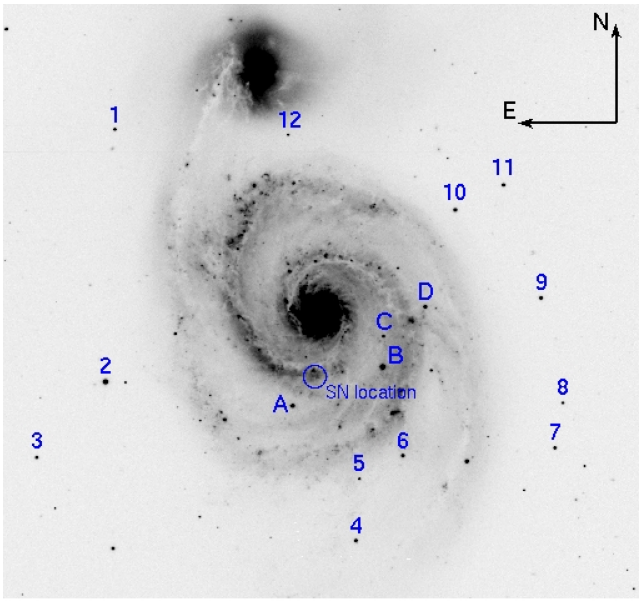

Figure 1. The Whirlpool galaxy (M51): *r*-band image obtained with the 2.56-m Isaac Newton Telescope on 2003 July 27 by M. Watson (ING Science Archive, http://casu.ast.cam.ac.uk/casuadc/archives/ingarch). The sequence of stars in the field of M51 used to calibrate the optical magnitudes of SN 2005cs is indicated. The four sequence stars used to calibrate the NIR photometry are marked with capital letters.

itself (Section 5.1) and in the context of the low-luminosity type IIP SN class (Section 5.2). Finally, in Section 6 we briefly summarize the main results of this paper.

2 PHOTOMETRY

The systematic photometric monitoring of SN 2005cs began on 2005 June 30, 3 d after the SN discovery. However, earlier unfiltered images obtained by amateur astronomers were also collected. These data are particularly important because they show the light-curve evolution soon after the shock breakout. There is no evidence of the SN presence in images obtained on 2005 June 26, but the SN was clearly visible the subsequent day (Fig. 2). The SN was then followed for one year (until 2006 July) in the optical bands, and until 2006 December in the NIR. A few optical observations obtained in 2007 show no trace of the SN.

Optical data were reduced following standard prescriptions in IRAF environment. Magnitude measurements were performed on the final images (i.e. after overscan, bias, flat-field correction) with a point spread function (PSF) fitting technique, after subtracting images of the host galaxy obtained before the SN explosion (for details about this technique see Sollerman et al. 2002). The calibration of the optical photometry was performed making use of standard fields of Landolt (1992) observed in the same nights as the SN. The SN magnitudes were then determined relative to the magnitudes of a sequence of stars in the field of M51 (Fig. 1, and Table 1), computed averaging the estimates obtained during several photometric nights. The calibrated SN magnitudes in optical bands are reported in Table 2.

Except for a few observations in the *B* band, most early-time amateur images were obtained without filters. However, we checked the quantum efficiency curves of all CCDs used in these observations and, depending on their characteristics, unfiltered measurements were rescaled to *V*- or *R*-band magnitudes (with the same prescriptions as in the case of the SN IIb 2008ax, see Pastorello et al. 2008), using the same local stellar sequence as for filtered photometry (Fig. 1 and Table 1). The calibrated magnitudes derived from amateur observations are listed in Table 3.

For the NIR photometry we used a slightly different approach. The contamination from the sky, which is extremely luminous and rapidly variable in the NIR, first had to be removed. To this aim, sky images, obtained by median-combining several exposures of relatively empty stellar fields,[1] were subtracted from individual SN frames. The final NIR images of the SN were obtained combining several dithered exposures. SN magnitudes were then computed with reference to a sequence of stars (labelled with capital letters in Fig. 1), whose magnitudes were calibrated using ARNICA NIR standard fields (Hunt et al. 1998, 2000) and that were found to be in good agreement with those of the 2MASS catalogue (see Table 1). NIR magnitudes of SN 2005cs are reported in Table 4.

2.1 The rising branch

After the collapse of the stellar nucleus, a shock wave travels from the core region outward, and reaches the outer envelope on timescales of hours. When the shock wave reaches regions of low optical depth, the SN begins to shine. This phenomenon is called shock breakout and is expected to manifest as a brief (few hours) burst of high-frequency (UV and X-ray) emission. Though theoretically expected, this sharp UV excess was only occasionally observed in type IIP SNe, and mostly during the post-peak decline. For example, the peculiar SN 1987A showed some evidence of it (Kirshner et al. 1987; Hamuy et al. 1988). The type IIP SN 2006bp was also discovered very young (Quimby et al. 2007), but not early enough to see the initial rise of the UV excess (Immler et al. 2007; Dessart et al. 2008). More recently, two other type IIP SNe discovered by the Supernova Legacy Survey were observed by *GALEX* soon after core-collapse and showed some evidence of a fast-rising UV light peak (Gezari et al. 2008; Schawinski et al. 2008). This sharp peak is much weaker (or totally invisible) in the optical bands, which only shows a relatively fast rise (2–3 d) to the plateau. Due to its intrinsic brevity, also the optical rising phase of a SN IIP was rarely observed in the past (e.g. Quimby et al. 2007).

SN 2005cs was discovered soon after its explosion (see Paper I), mainly because M51 is one of the most frequently targeted nearby galaxies by amateur astronomers. For this reason, a number of images obtained shortly before (and soon after) core-collapse are available. We analysed several of these images, and derived a number of significant pre-explosion limits and the very early-time *B*-, *V*- and *R*-band photometry of SN 2005cs (Fig. 3). These measurements, obtained around the discovery epoch, provide a robust constraint on the epoch of the explosion and the rare opportunity to observe the fast rise to the light-curve maximum of a type II SN. The non-detection at JD = 245 3548.43 and the detection at JD = 245 3549.41 allow us to estimate the time of the shock breakout to be around JD = 245 3549.0 ± 0.5 (this epoch corresponds to day 0 in Fig. 3 and hereafter). As pointed out by Dessart et al. (2008), there is a time interval elapsing between the beginning of the expansion (computed by Dessart et al. 2008, JD = 245 3547.6) and the instant of the optical brightening.

[1] Sky images are usually obtained a short time apart the SN observations, pointing the telescope towards a relatively empty sky region, which has to be relatively close (a few arcminutes far away) from the SN coordinates.

Table 1. Magnitudes of the sequence stars in the SN field (see Fig. 1). The errors are the rms of the average magnitudes.

Star	*U*	*B*	*V*	*R*	*I*	*z*	*J*	*H*	*K*
1		17.012 (0.176)	16.274 (0.029)	15.812 (0.079)	15.436 (0.062)				
2	14.617 (0.043)	14.317 (0.020)	13.601 (0.015)	13.188 (0.013)	12.815 (0.008)				
3	17.328 (0.178)	16.555 (0.015)	15.686 (0.056)	15.121 (0.013)	14.622 (0.023)				
4	16.147 (0.053)	16.235 (0.023)	15.659 (0.020)	15.228 (0.015)	14.915 (0.033)				
5	18.881 (0.071)	18.254 (0.066)	17.362 (0.014)	16.750 (0.016)	16.281 (0.015)				
6	15.511 (0.017)	15.848 (0.011)	15.394 (0.021)	15.049 (0.009)	14.744 (0.011)				
7	17.133 (0.192)	16.730 (0.013)	16.063 (0.017)	15.541 (0.012)	15.097 (0.047)				
8	19.764 (0.021)	18.718 (0.048)	17.412 (0.040)	15.818 (0.027)	14.378 (0.034)				
9	18.008 (0.232)	16.662 (0.027)	15.675 (0.015)	14.975 (0.010)	14.355 (0.038)				
10	16.743 (0.036)	16.197 (0.030)	15.285 (0.010)	14.746 (0.022)	14.198 (0.021)				
11	19.258 (0.040)	17.574 (0.037)	16.151 (0.014)	15.058 (0.018)	13.902 (0.040)				
12	18.055 (0.106)	18.044 (0.060)	17.409 (0.018)	16.948 (0.026)	16.613 (0.071)				
A	17.773 (0.030)	16.343 (0.009)	15.107 (0.006)	14.334 (0.011)	13.681 (0.008)	13.344 (0.024)	12.846 (0.034)	12.248 (0.008)	12.142 (0.041)
B	14.120 (0.023)	14.007 (0.009)	13.433 (0.005)	13.061 (0.005)	12.726 (0.009)	12.563 (0.019)	12.285 (0.011)	11.970 (0.022)	11.950 (0.009)
C	17.186 (0.036)	17.149 (0.018)	16.667 (0.011)	16.292 (0.012)	15.941 (0.014)	15.818 (0.052)	15.467 (0.033)	15.009 (0.017)	15.062 (0.045)
D	15.757 (0.026)	15.773 (0.010)	15.244 (0.008)	14.853 (0.007)	14.517 (0.008)	14.370 (0.033)	14.070 (0.012)	13.745 (0.064)	13.738 (0.030)

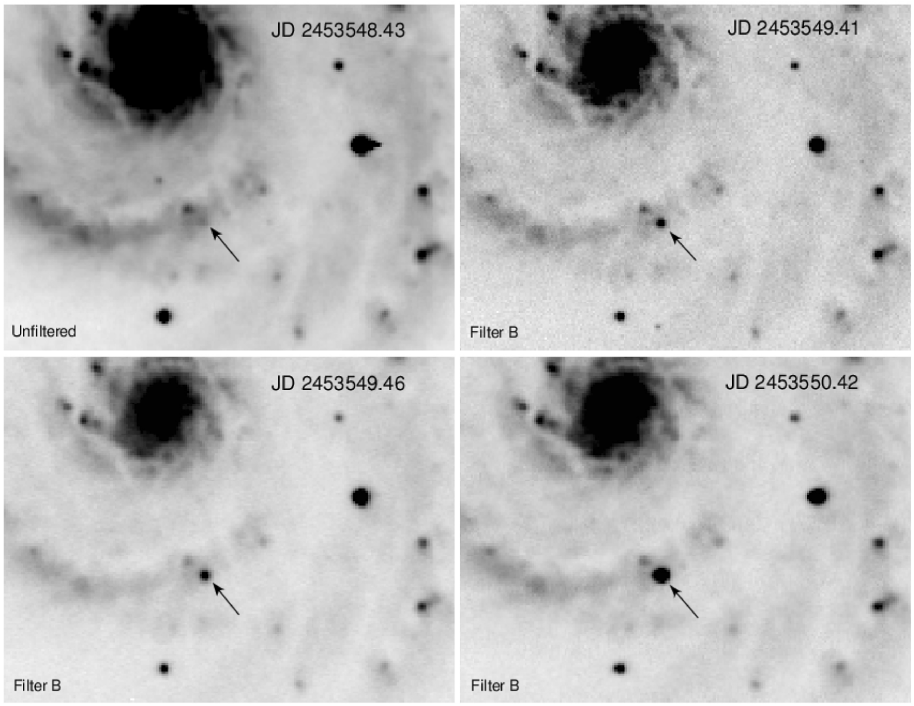

Figure 2. Images of the site of explosion of SN 2005cs between 2005 June 26 and 28, taken by M. Fiedler with his 0.35-m Telescope. The first unfiltered image (top left-hand panel, resulting from the combination of 10 individual images of 600 s each) was obtained on June 26 at an average UT = 22.3, which is near the expected time of the shock breakout. The other *B*-band images, obtained during the subsequent 2 d, show the rapid brightening of SN 2005cs.

Remarkably, the sharp peak of light soon after core-collapse mentioned by Tsvetkov et al. (2006) and shown in their fig. 4, is *not visible* in our calibrated photometry (see Fig. 3). This putative peak was likely an artefact due to the lack of selection criteria in collecting unfiltered observations from a large number of amateur astronomers. For comparison, in Fig. 3 the rising phase of the normal type IIP SN 2006bp, as presented in Quimby et al. (2007), is also shown. The behaviour of these two objects suggests that the rise to the maximum light is extremely rapid in SNe IIP, lasting about 2 d, and it is much faster than that observed in other SN types.

2.2 The plateau phase

Optical and NIR light curves of SN 2005cs obtained during the first 4 months (including also the amateurs observations discussed in Section 2.1) are shown in Fig. 4. The black symbols are original data presented in this paper plus the data of Paper I recalibrated with the new sequence of stars, while the red ones are from Tsvetkov et al. (2006). Evidence of a maximum light is visible only in the *U*- and *B*-band light curves (and also in the UV observations presented by Brown et al. 2007). In the other optical bands SN 2005cs

Table 2. *UBVRIz* magnitudes of SN 2005cs and assigned errors, which account for both measurement errors and uncertainties in the photometric calibration. The observations presented in Paper I are also reported, recalibrated with the new sequence of stars identified in Fig. 1.

Date dd/mm/yy	JD (+240 0000)	*U*	*B*	*V*	*R*	*I*	*z*	Instrument
23/04/05	53483.59			>19.8				1
30/06/05	53552.36	13.460 (0.008)	14.393 (0.009)	14.496 (0.011)	14.459 (0.016)	14.455 (0.016)		2
01/07/05	53553.35	13.448 (0.012)	14.410 (0.023)	14.531 (0.026)	14.435 (0.018)	14.369 (0.028)		3
02/07/05	53554.46	13.573 (0.014)	14.470 (0.020)	14.541 (0.010)	14.460 (0.017)	14.336 (0.012)		3
03/07/05	53555.49		14.488 (0.015)	14.541 (0.008)	14.380 (0.009)			1
05/07/05	53557.42		14.553 (0.026)	14.549 (0.027)	14.396 (0.024)	14.333 (0.056)		3
05/07/05	53557.44			14.497 (0.016)	14.375 (0.008)			1
06/07/05	53557.84	13.997 (0.018)	14.580 (0.029)	14.578 (0.019)	14.350 (0.018)	14.462 (0.012)		4
07/07/05	53559.40		14.624 (0.024)	14.575 (0.083)	14.393 (0.080)	14.359 (0.105)		5
10/07/05	53562.43		14.829 (0.012)					6
11/07/05	53563.38	14.735 (0.008)	14.904 (0.006)	14.603 (0.007)	14.355 (0.008)	14.229 (0.008)		3
11/07/05	53563.42	14.750 (0.011)	14.911 (0.010)	14.575 (0.009)	14.355 (0.011)	14.251 (0.013)		7
13/07/05	53565.38	15.292 (0.030)	15.046 (0.020)	14.652 (0.013)	14.360 (0.014)	14.287 (0.018)	14.215 (0.020)	6
13/07/05	53565.45		15.056 (0.014)	14.648 (0.011)	14.368 (0.021)			1
14/07/05	53566.36	15.263 (0.012)	15.115 (0.010)	14.684 (0.010)	14.389 (0.018)	14.229 (0.013)		3
14/07/05	53566.40		15.092 (0.025)	14.666 (0.027)	14.380 (0.016)	14.282 (0.025)		5
17/07/05	53569.42	15.994 (0.034)	15.345 (0.017)	14.723 (0.019)	14.382 (0.016)	14.273 (0.022)	14.192 (0.021)	6
19/07/05	53571.40		15.374 (0.025)	14.724 (0.020)	14.454 (0.019)	14.258 (0.028)		5
20/07/05	53572.40		15.389 (0.037)	14.723 (0.027)	14.447 (0.020)	14.282 (0.019)		5
25/07/05	53577.40		15.489 (0.078)	14.746 (0.039)	14.327 (0.059)	14.239 (0.045)		5
27/07/05	53579.40		15.605 (0.046)	14.754 (0.037)	14.394 (0.030)	14.167 (0.025)		5
31/07/05	53583.39	16.741 (0.065)	15.758 (0.022)	14.750 (0.015)	14.334 (0.014)	14.118 (0.013)		7
31/07/05	53583.47	16.746 (0.077)	15.768 (0.037)	14.755 (0.012)	14.325 (0.012)	14.164 (0.012)	13.999 (0.011)	6
02/08/05	53585.38		15.772 (0.075)	14.753 (0.064)	14.327 (0.038)	14.099 (0.026)		8
02/08/05	53585.40		15.798 (0.009)	14.764 (0.008)	14.328 (0.006)	14.129 (0.008)		6
03/08/05	53586.43	16.940 (0.048)	15.839 (0.014)	14.750 (0.012)	14.271 (0.010)	14.089 (0.010)	13.956 (0.010)	6
05/08/05	53588.38		15.850 (0.017)	14.769 (0.010)	14.267 (0.006)	14.096 (0.007)		6
06/08/05	53589.38	17.040 (0.093)	15.890 (0.015)	14.767 (0.009)	14.263 (0.008)	14.094 (0.010)	13.930 (0.010)	6
10/08/05	53593.42	17.166 (0.184)	15.934 (0.018)	14.784 (0.015)	14.285 (0.011)	13.962 (0.010)		7
12/08/05	53595.38		15.969 (0.021)	14.778 (0.010)	14.241 (0.012)	14.009 (0.008)		6
12/08/05	53595.39	17.244 (0.077)	15.960 (0.012)	14.776 (0.010)	14.241 (0.011)	13.983 (0.009)	13.847 (0.010)	6
16/08/05	53599.44		16.009 (0.037)	14.772 (0.013)	14.211 (0.004)	13.967 (0.004)		6
17/08/05	53600.41		16.012 (0.035)	14.768 (0.006)	14.206 (0.020)			1
22/08/05	53605.35		16.088 (0.061)	14.745 (0.019)	14.198 (0.021)	13.946 (0.020)	13.774 (0.017)	6
22/08/05	53605.42		16.095 (0.026)	14.761 (0.014)	14.198 (0.010)	13.922 (0.010)		6
23/08/05	53606.42		16.110 (0.034)	14.771 (0.009)	14.164 (0.011)	13.886 (0.009)		6
27/08/05	53610.34	17.601 (0.210)	16.105 (0.029)	14.734 (0.011)	14.139 (0.009)	13.906 (0.010)	13.729 (0.008)	6
27/08/05	53610.37		16.102 (0.019)	14.724 (0.008)	14.150 (0.008)	13.903 (0.008)		6
27/08/05	53610.40	17.586 (0.102)	16.070 (0.018)	14.793 (0.015)	14.181 (0.015)	13.944 (0.015)		7
30/08/05	53613.34		16.099 (0.078)	14.730 (0.028)	14.149 (0.030)	13.838 (0.023)	13.687 (0.024)	6
30/08/05	53613.35		16.107 (0.047)	14.732 (0.012)	14.122 (0.010)	13.886 (0.023)		6
01/09/05	53615.33		16.116 (0.026)	14.752 (0.018)	14.122 (0.011)			1
01/09/05	53615.35		16.128 (0.034)	14.765 (0.016)	14.128 (0.012)	13.874 (0.012)		6
03/09/05	53617.35	17.636 (0.190)	16.140 (0.034)	14.768 (0.013)	14.171 (0.015)	13.840 (0.018)	13.670 (0.013)	6
05/09/05	53619.35	17.669 (0.270)	16.138 (0.035)	14.778 (0.016)	14.155 (0.011)	13.853 (0.013)	13.681 (0.016)	6
14/09/05	53628.35	17.718 (0.300)	16.194 (0.039)	14.838 (0.011)	14.110 (0.010)	13.801 (0.009)	13.641 (0.014)	6
10/10/05	53654.26		16.574 (0.230)			13.942 (0.041)		3
11/10/05	53655.28		16.608 (0.237)	15.109 (0.076)		13.959 (0.024)		3
16/10/05	53660.28		16.815 (0.027)	15.156 (0.041)	14.430 (0.007)			1
16/10/05	53660.31		16.822 (0.092)					1
18/10/05	53662.26		16.872 (0.122)	15.218 (0.013)	14.488 (0.009)			1
28/10/05	53671.67		18.099 (0.110)	16.055 (0.049)	15.067 (0.012)			1
29/10/05	53672.68		18.450 (0.033)	16.260 (0.045)	15.134 (0.030)	14.576 (0.021)		3
04/11/05	53678.64		>19.60	18.825 (0.280)	17.419 (0.042)			1
05/11/05	53679.77	>19.93	21.053 (0.290)	18.870 (0.176)	17.483 (0.089)	16.673 (0.078)	15.943 (0.280)	6
07/11/05	53681.76	>18.68	>19.34	18.864 (0.330)	17.422 (0.122)	16.656 (0.044)	15.916 (0.104)	6
08/11/05	53682.65			18.929 (0.086)	17.441 (0.040)			3
09/11/05	53683.70		21.132 (0.290)	19.063 (0.067)	17.460 (0.042)			3
09/11/05	53683.76	>18.21			17.530 (0.032)			6
11/11/05	53685.77			19.256 (0.160)	17.547 (0.052)			6

Table 2 – *continued*

Date dd/mm/yy	JD (+240 0000)	*U*	*B*	*V*	*R*	*I*	*z*	Instrument
13/11/05	53687.78				17.556 (0.088)			6
25/11/05	53699.72		21.393 (0.530)	19.280 (0.440)	17.859 (0.103)	16.984 (0.193)	16.204 (0.420)	6
02/12/05	53706.71		21.511 (0.340)	19.448 (0.075)	18.007 (0.024)			1
03/12/05	53707.74			19.429 (0.120)		17.096 (0.061)		6
03/12/05	53707.75		21.562 (0.470)	19.435 (0.095)		17.051 (0.163)	16.196 (0.450)	6
05/12/05	53709.74		21.545 (0.244)	19.433 (0.174)	17.875 (0.045)	17.062 (0.095)	16.285 (0.051)	6
12/12/05	53715.57		21.636 (0.430)		17.871 (0.148)	17.195 (0.095)		3
14/12/05	53718.69		>20.34	19.524 (0.102)	17.959 (0.042)	17.191 (0.048)		6
22/12/05	53725.72		21.632 (0.350)	19.542 (0.115)		17.261 (0.063)		3
27/12/05	53731.64			19.563 (0.220)	18.077 (0.078)	17.237 (0.047)		6
31/12/05	53735.62			19.577 (0.184)	18.130 (0.122)	17.290 (0.032)		6
15/01/06	53750.74			19.479 (0.220)				1
03/02/06	53769.54		>20.30					6
03/02/06	53769.72			19.525 (0.079)				1
04/02/06	53770.57			19.610 (0.044)	18.380 (0.111)	17.523 (0.038)		6
08/02/06	53774.63		21.774 (0.250)	19.613 (0.102)	18.550 (0.043)	17.645 (0.081)		3
20/02/06	53786.57			19.642 (0.052)	18.578 (0.136)	17.749 (0.052)		6
06/03/06	53800.57			19.708 (0.420)	18.604 (0.053)	17.879 (0.310)		6
19/03/06	53814.46		21.823 (0.210)					6
20/03/06	53815.45			19.707 (0.100)	18.605 (0.034)	17.880 (0.082)		6
24/03/06	53818.63			19.727 (0.046)	18.630 (0.034)	17.920 (0.090)		7
04/04/06	53830.46			19.808 (0.094)	18.667 (0.041)	17.951 (0.036)		6
19/04/06	53845.40			19.896 (0.046)	18.757 (0.063)	18.023 (0.039)		6
03/05/06	53859.42		22.033 (0.320)					6
04/05/06	53860.41			20.001 (0.087)	18.964 (0.064)	18.182 (0.058)		6
15/05/06	53871.67			20.128 (0.119)	18.983 (0.225)	18.217 (0.110)		6
17/06/06	53904.51			20.355 (0.081)	19.437 (0.091)	18.545 (0.050)		6
09/07/06	53926.43			20.679 (0.200)	19.505 (0.280)	18.967 (0.240)		6
30/01/07	54130.56			>22.42	>21.99	>20.69		7

1 = 0.8-m Wendelstein Telescope + MONICA (University Observatory Munich, Mt Wendelstein, Germany);
2 = 2.2-m Calar Alto Telescope + CAFOS (German-Spanish Astronomical Center, Sierra de Los Filabres, Andalucía, Spain);
3 = 1.82-m Copernico Telescope + AFOSC (INAF – Osservatorio Astronomico di Asiago, Mt Ekar, Asiago, Italy);
4 = 8.2-m Subaru Telescope + FOCAS (National Astronomical Observatory of Japan, Mauna Kea, Hawaii, US);
5 = 0.72-m Teramo-Normale Telescope + CCD camera (INAF – Osservatorio Astronomico di Collurania, Teramo, Italy);
6 = 2.0-m Liverpool Telescope + RatCAM (La Palma, Spain);
7 = 3.58-m Telescopio Nazionale Galileo + Dolores (Fundación Galileo Galilei – INAF, La Palma, Spain);
8 = 1.52-m Cassini Telescope + BFOSC (INAF – Osservatorio Astronomico di Bologna, Loiano, Italy).

shows a long period (more than 100 d) of almost constant luminosity (especially in the *V* band). Unlike the optical light curves, in the NIR the luminosity increases monotonically until the end of the plateau. We note that a plateau of 100–120 d is a common feature of most SNe IIP (see also the systematic analysis in Höflich et al. 2001; Hamuy 2003; Nadyozhin 2003; Chieffi et al. 2003).

During the plateau phase the massive H-rich envelope, which was fully ionized at the time of the initial shock breakout, cools and recombines. During this period the SN becomes progressively redder. Multiple colour curves of SN 2005cs during the first few months are shown in Fig. 5 and compared with those of a few well observed SNe IIP: the peculiar SN 1987A (see Whitelock et al. 1989, and references therein), the normal luminosity SN 1999em (Hamuy et al. 2001; Leonard et al. 2002b; Elmhamdi et al. 2003a; Krisciunas et al. 2009), and the low-luminosity SNe 1999br and 1999eu (Hamuy 2003; Pastorello et al. 2004). All SNe IIP show a similar colour evolution, becoming monotonically redder with time, even though the peculiar SN 1987A reddens definitely faster than the others. Conversely, no significant colour evolution is visible during the plateau phase in the NIR, with the $J - H$ colour being constant at $\sim$0.2 mag and the $J - K$ colour at $\sim$0.25 mag.

After the end of recombination (about four months after core-collapse), the SN luminosity drops abruptly (Fig. 6) and the colour curves show a red peak (see Section 2.3 and Fig. 7) previously observed in other type IIP SNe (Pastorello et al. 2004; Hendry et al. 2005). SN 2005cs declines by about 4.5 mag within 3 weeks in the *B* band, by $\sim$3.8 mag in the *V* band, $\sim$3.1 mag in the *R* band, $\sim$2.7 mag in the *I* band and $\sim$2.3 mag in *z* band. This drop is unusually large, since in most type IIP SNe it is in the range 1.5–3 mag (see e.g. Elmhamdi, Chugai & Danziger 2003b).

2.3 The nebular phase

Once the H envelope is fully recombined, SN 2005cs is expected to approach the nebular phase. In this phase, its luminosity is sustained only by the radioactive decay of iron-group elements. Under the assumption of complete γ-ray trapping, the light curve is expected to decline with a rate of 0.98 mag/100 d, consistent with the decay of ^{56}Co into ^{56}Fe. In Fig. 6 we show the late-time optical photometry of SN 2005cs. It is worth noting that the post-plateau photometric data of Tsvetkov et al. (2006), considered by the authors as preliminary, are not shown in Fig. 6 because

Table 3. Early time *BVR* magnitudes of SN 2005cs from amateur observations. The errors take into account both measurement errors and uncertainties in the photometric calibration. The *B*-band magnitudes are derived from filtered images. All other images were unfiltered, but rescaled to the *V*- or *R*-band photometry depending on the peak of the quantum-efficiency curve of the detectors used by the amateurs (see also the discussion in Pastorello et al. 2008).

Date dd/mm/yy	JD (+240 0000)	*B*	*V*	*R*	Instrument
19/06/05	53540.55			>17.0	A
25/06/05	53547.44			>18.4	B
26/06/05	53548.39	>17.3	>17.7	>17.6	C†
26/06/05	53548.43			>19.7	D
27/06/05	53549.41	16.728 (0.122)			D†
27/06/05	53549.42		16.367 (0.330)		E
27/06/05	53549.43			16.301 (0.073)	F
27/06/05	53549.43		16.250 (0.161)		G
27/06/05	53549.44			16.302 (0.086)	F
27/06/05	53549.45	16.375 (0.145)			D†
27/06/05	53549.46	16.319 (0.153)			D†
27/06/05	53549.46		16.224 (0.278)		E
27/06/05	53549.49			16.214 (0.154)	H
28/06/05	53550.41	14.677 (0.124)			D†
28/06/05	53550.42	14.654 (0.148)			D†
28/06/05	53550.43		14.872 (0.150)		G
30/06/05	53551.51			14.475 (0.170)	H
30/06/05	53552.37		14.499 (0.150)		I
30/06/05	53552.44		14.493 (0.222)		J
30/06/05	53552.46		14.491 (0.165)		G
30/06/05	53552.46		14.495 (0.174)		G
01/07/05	53552.56		14.498 (0.155)		G
01/07/05	53553.46		14.527 (0.169)		I
02/07/05	53554.46		14.538 (0.146)		J
03/07/05	53555.44		14.539 (0.085)		J
03/07/05	53555.48		14.552 (0.046)		G
06/07/05	53558.44			14.334 (0.130)	F
08/07/05	53560.42			14.358 (0.121)	F
08/07/05	53560.48		14.586 (0.086)		G
09/07/05	53561.43		14.588 (0.075)		G
10/07/05	53562.47		14.600 (0.093)		G
12/07/05	53564.44		14.593 (0.082)		G
13/07/05	53565.43		14.628 (0.107)		G
14/07/05	53566.47		14.663 (0.071)		G
15/07/05	53567.46		14.692 (0.239)		G
17/07/05	53569.40		14.731 (0.073)		G
19/07/05	53571.45		14.724 (0.241)		G
20/07/05	53572.41		14.724 (0.148)		G

†Photometry obtained from images with filters.

A = 80-mm Skywatcher ED80 Refractor Telescope + SBIG ST-7 Dual CCD Camera with KAF-0400 (I. Uhl, Rheinzabern, Germany);

B = 0.2-m Orion SVP Reflector Telescope + Starlight Xpress MX5C CCD Camera (C. McDonnell, Holliston, Massachusetts, US);

C = 0.4-m Newton Telescope + ERG110 CCD (Osservatorio Astronomico Geminiano Montanari, Cavezzo, Modena, Italy);

D = 0.35-m Maksutov Newtonian Reflector Telescope + SBIG ST10XME CCD Camera with KAF-3200ME (M. Fiedler, Astroclub Radebeul, Germany);

E = 0.356-m Celestron 14 CGE Telescope + SBIG ST-2000 CCD (P. Marek, Skymaster Observatory, Variable Star Section of Czech Astronomical Society, Borovinka, Czech Republic);

F = 0.4-m Meade Schmidt-Cassegrain Telescope + Marconi (E2V) CCD 47-10 (P. Birtwhistle, Great Shefford Observatory, West Berkshire, England);

G = 0.203-m f/4.0 Meade Newtonian Reflector Telescope + DSI-Pro II CCD Camera (W. Kloehr, Schweinfurt, Germany);

H = 0.28-m Celestron 11 + MX7-C CCD (U. Bietola, Gruppo Imperiese Astrofili, Imperia, Italy);

I = 0.20-m Celestron 8 SCT + Starlight Xpress MX916 CCD (P. Corelli, Mandi Observatory, Pagnacco, Udine, Italy);

J = 0.25-m Newton f/4.8 Telescope + StarLight Xpress SXL8 CCD (T. Scarmato, Toni Scarmato's Observatory, San Costantino di Briatico, Vibo Valentia, Italy).

Table 4. *JHK* magnitudes of SN 2005cs and assigned errors, which take into account both measurement errors and uncertainties in the photometric calibration.

Date dd/mm/yy	JD (+240 0000)	*J*	*H*	*K*	Instrument
02/07/05	53554.38	14.434 (0.052)	14.170 (0.031)		1
11/07/05	53563.41	14.202 (0.075)	13.813 (0.068)	13.848 (0.085)	1
21/07/05	53573.39	13.980 (0.022)	13.742 (0.045)		1
22/07/05	53574.45			13.637 (0.073)	1
24/07/05	53575.53	13.910 (0.022)	13.690 (0.013)	13.621 (0.022)	2
27/07/05	53579.44	13.901 (0.028)	13.668 (0.039)	13.652 (0.109)	1
28/07/05	53580.40	13.887 (0.028)	13.699 (0.105)	13.623 (0.157)	1
01/08/05	53584.42	13.843 (0.031)	13.626 (0.037)	13.557 (0.065)	1
02/08/05	53585.33	13.814 (0.027)	13.608 (0.058)	13.549 (0.160)	1
08/08/05	53591.36	13.717 (0.057)	13.507 (0.039)	13.398 (0.058)	1
23/08/05	53606.33	13.553 (0.022)	13.392 (0.023)	13.287 (0.028)	1
27/08/05	53610.38	13.521 (0.008)	13.357 (0.019)	13.242 (0.039)	2
29/08/05	53612.32	13.515 (0.013)	13.352 (0.018)		1
30/08/05	53613.32			13.256 (0.031)	1
10/09/05	53624.31	13.500 (0.018)	13.251 (0.028)		1
12/09/05	53626.26	13.474 (0.033)	13.249 (0.029)	13.240 (0.037)	1
15/09/05	53629.29	13.463 (0.058)	13.258 (0.041)	13.186 (0.029)	1
26/09/05	53640.27	13.517 (0.019)	13.257 (0.046)	13.140 (0.039)	1
28/09/05	53642.28	13.530 (0.032)	13.228 (0.053)	13.159 (0.030)	1
14/02/06	53781.48	17.222 (0.220)		16.452 (0.380)	1
24/03/06	53818.74	17.621 (0.137)	17.354 (0.169)	17.119 (0.119)	2
26/11/06	54065.67	18.114 (0.320)	17.809 (0.450)		1
01/12/06	54070.66	18.129 (0.310)			1
02/12/06	54071.66			17.428 (0.320)	1

1 = 1.08-m AZT24 Telescope + SWIRCAM (Pulkovo Observatory, St Petersburg, Russia + INAF-Osservatori Astronomici di Roma and Teramo, Stazione di Campo Imperatore, Italy);
2 = 3.58-m Telescopio Nazionale Galileo + NICS (Fundación Galileo Galilei – INAF, La Palma, Spain).

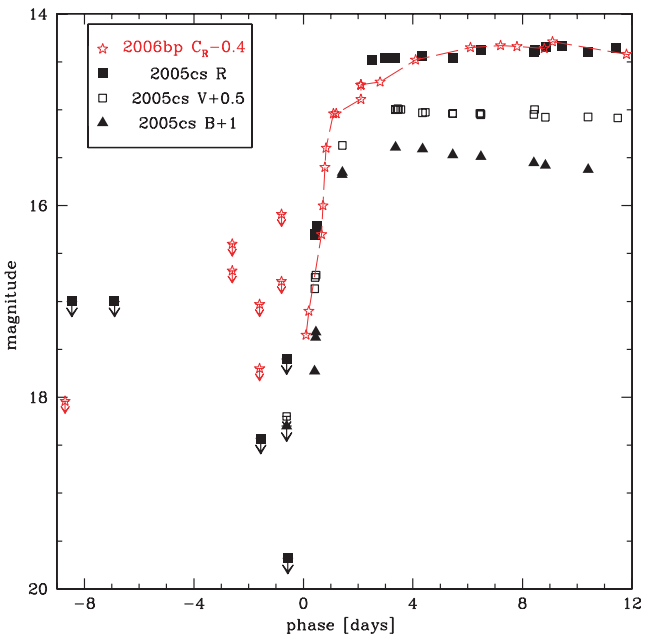

Figure 3. SN 2005cs in M51: the rising branch of the optical light curves, compared with SN 2006bp (Nakano & Itagaki 2006; Quimby et al. 2007). The phase is computed from the adopted time of the shock breakout (JD = 245 3549.0 ± 0.5). A detection limit obtained on June 20 by K. Itagaki ($R > 17.0$, see Kloehr et al. 2005) is also shown.

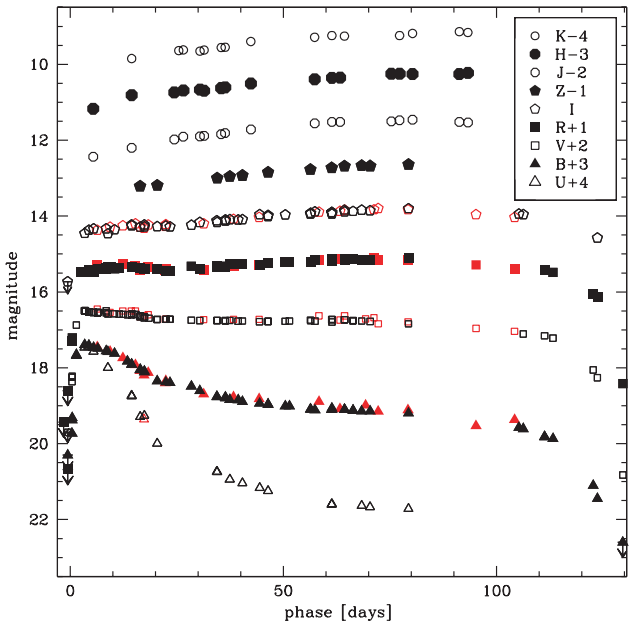

Figure 4. SN 2005cs in M51: *UBVRIzJHK* light curves during the plateau phase. The early-time optical photometry of Tsvetkov et al. (2006) is also reported, with red symbols.

they are systematically brighter than those presented in this paper. This is probably due to the different methods used to derive the magnitudes. In fact, when the SN luminosity is comparable to that of the local background, the photometry without template subtraction

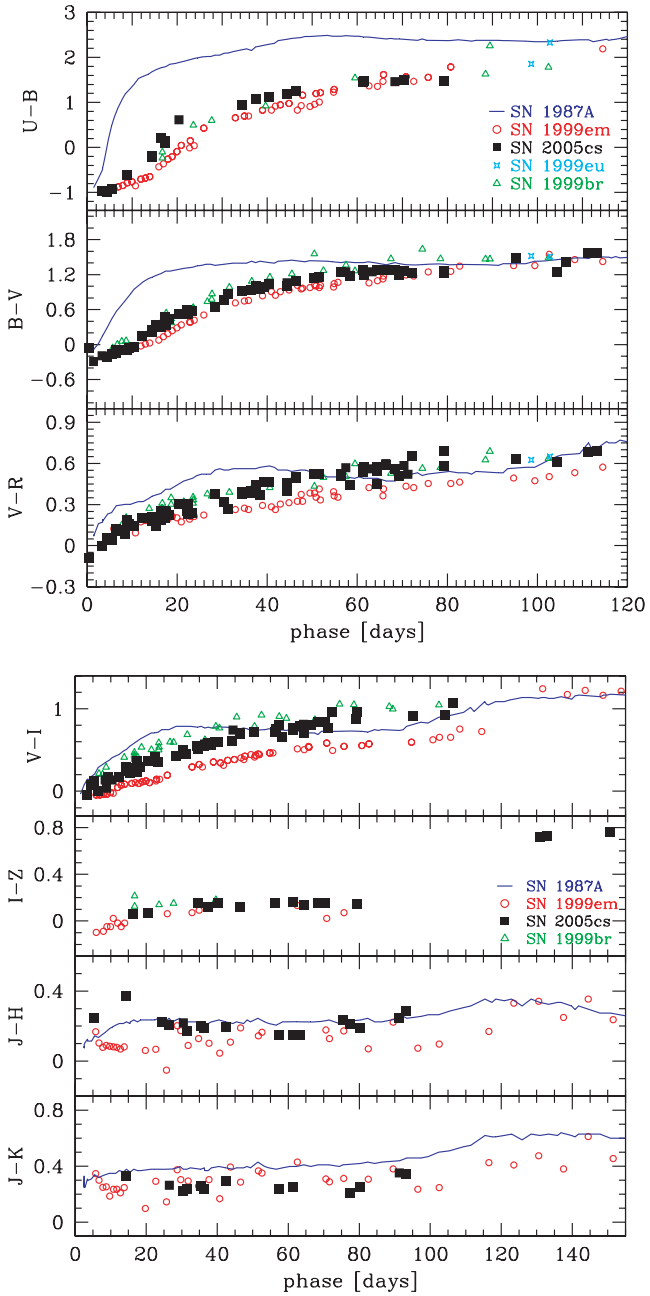

Figure 5. SN 2005cs in M51: $U-B$, $B-V$ and $V-R$ (top panel, during the plateau phase) and $V-I$, $I-z$, $J-H$, $J-K$ colour curves (bottom panel, up to 155 d), and comparison with the type IIP SNe 1987A (Whitelock et al. 1989, and references therein), 1999em (Hamuy et al. 2001; Leonard et al. 2002b; Elmhamdi et al. 2003a; Krisciunas et al. 2009), 1999eu (Pastorello et al. 2004) and 1999br (Hamuy 2003; Pastorello et al. 2004).

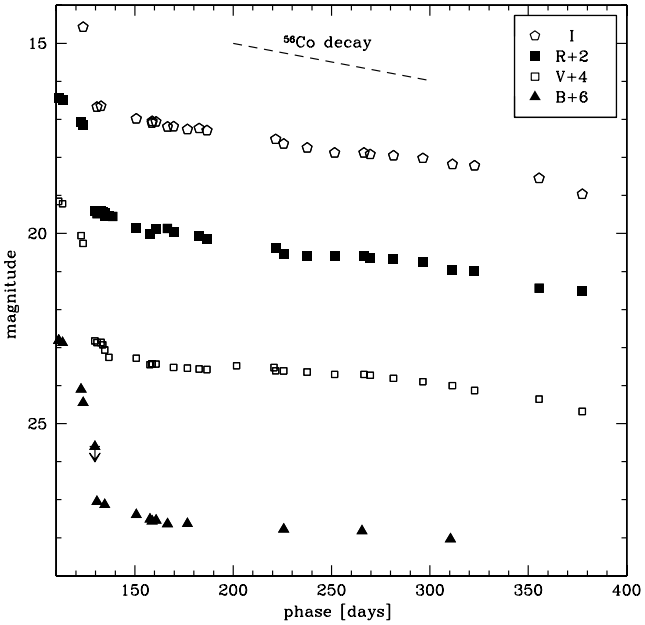

Figure 6. SN 2005cs in M51: *BVRI* light curves during the nebular phase. The typical slope of the ^{56}Co decay to ^{56}Fe (in the case of complete γ-ray trapping) is also indicated by a dashed line.

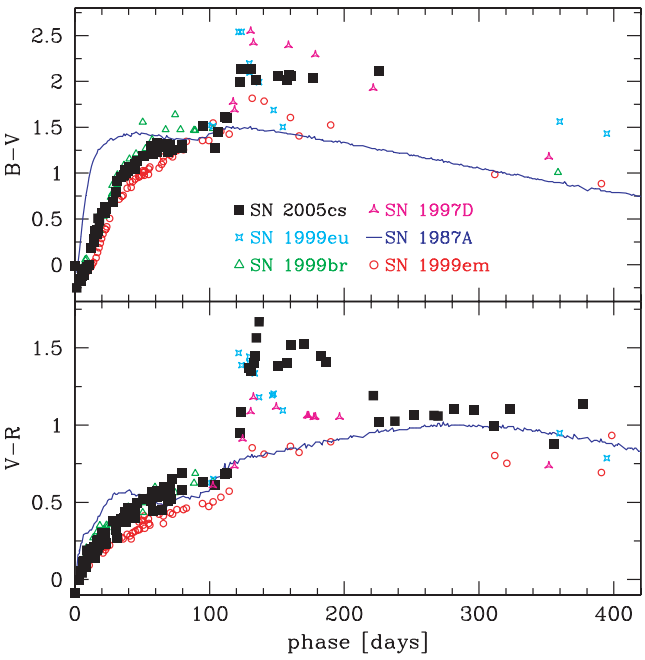

Figure 7. SN 2005cs in M51: $B-V$ (top) and $V-R$ (bottom) colour curves from early-time to the nebular phase. SN 2005cs is compared to the sample of type IIP SNe from Fig. 5 and the prototypical low-luminosity SN 1997D (Turatto et al. 1998; Benetti et al. 2001).

no longer provides good results. For this reason we subtracted the host galaxy using archival images obtained before the SN explosion. Comparing our V-band magnitudes of the radioactive tail obtained with the template subtraction with those of Tsvetkov et al. (2006), we find differences as large as 1 mag. This is not surprising, since SN 2005cs at late phases emits mostly at red wavelengths and, hence, the V-band magnitude estimates from Tsvetkov et al. (2006) are expected to be significantly contaminated by the contribution of foreground sources. Once more, the subtraction of the host galaxy is crucial to get reliable magnitude estimates when the SN fades in luminosity.

The decline rates of SN 2005cs in the different bands during the period 140–320 d (Fig. 6) are: $\gamma_B = 0.32$, $\gamma_V = 0.46$, $\gamma_R = 0.71$ and $\gamma_I = 0.77$ mag/100 d. These are all significantly smaller than the decline rate expected from the ^{56}Co decay. Utrobin (2007) describes a transitional phase in the light-curve evolution of SNe IIP

where the luminosity does not fall directly on to the radioactive tail because of a residual contribution from radiation energy. According to Utrobin (2007), a radiation flow generated in the warmer inner ejecta propagates throughout the transparent cooler external layers, and contributes to the light curve as an additional source. One can observe this phase as a sort of late-time plateau (labelled as *plateau tail phase* by Utrobin 2007), before the light curves approaches the proper, uncontaminated radioactive decay phase. This transitional period is observed in many SNe IIP. A flattening in the early nebular tail was observed in the light curve of SN 1999em (Elmhamdi et al. 2003a), lasting less than one month (as estimated by Utrobin 2007, for a normal SN IIP). This phenomenon appears much more evident in underluminous, low-energy events (e.g. this late light-curve flattening was clearly observed in SN 1999eu; Pastorello et al. 2004). The situation for SN 2005cs is similar to that of SN 1999eu, since the secondary, late-time plateau lasts for about 6 months (possibly showing some substructures, like a step visible in Fig. 6 around 220 d). This, together with the evidence that P-Cygni photospheric lines are persistent in the SN spectra over a period of almost one year (see Section 4.1), indicates that the transition to the 'genuine' nebular phase is very slow in SN 2005cs and, probably, also in most other underluminous SNe IIP.

At very late epochs ($t > 330$ d) the SN luminosity declines faster. This is possibly an indication of (i) dust forming in the SN ejecta, (ii) a lower efficiency of γ-ray trapping due to the decreased density of the ejecta, or – more likely – (iii) that the residual luminosity contribution from radiation energy is vanishing and the light curve of SN 2005cs is finally settling on to the 'true' radioactive tail (Utrobin 2007). The measured slope of the light curve after ∼330 d is close indeed to that expected from the ^{56}Co decay (see Fig. 6). Further constraints can be obtained through the analysis of the nebular spectra (Section 4.1).

The comprehensive $B - V$ and $V - R$ colour curves of SN 2005cs and other SNe IIP (the same as in Fig. 5, but extended until 1 yr after core-collapse, and including those of the reference low-luminosity SN IIP 1997D) are shown in Fig. 7. SN 2005cs, like other faint SNe IIP (Pastorello et al. 2004; Spiro et al., in preparation), shows a characteristic red peak in the colour evolution during the steep post-plateau luminosity decline. However, while $B - V$ is constant at about 2 mag during the subsequent period, the $V - R$ colour (which peaks around 1.6 mag) becomes slightly bluer when the SN settles down on to the exponential tail, reaching $V - R \approx 1.2$. Note, however, that the faintness of SN 2005cs at the blue wavelengths at late phases makes the corresponding colour estimates rather uncertain.

3 BOLOMETRIC LIGHT CURVE AND NI MASS

Using the data presented in the previous sections, and early-time data of Tsvetkov et al. (2006) and Brown et al. (2007), we computed the bolometric light curve of SN 2005cs. The bolometric luminosity was calculated only for epochs in which *V*-band observations were available. Photometric data in the other optical bands, if not available at coincident epochs, were estimated interpolating the data of adjacent nights. Lacking NIR observations between 3 and 7 months after the SN explosion (i.e. during the period of the transition between the photospheric and the nebular phase), the contribution in the z, J, H and K bands was estimated by interpolating the $I - z$, $z - J$, $J - H$ and $H - K$ colour curves, respectively, with low-order polynomial functions. With this approach we can extrapolate information on the behaviour of the NIR light curves in the missing epochs. The colour curves of type IIP SNe, indeed, evolve

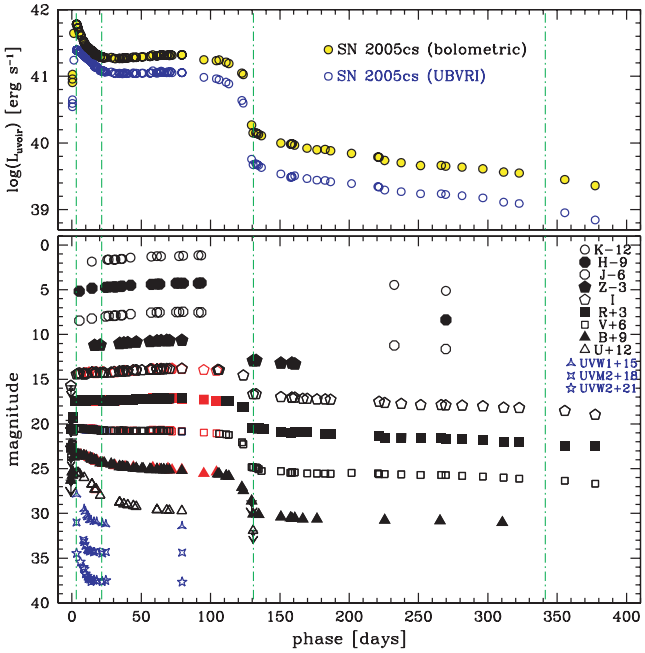

Figure 8. SN 2005cs in M51: Top: quasi-bolometric (*UBVRI*) light curve of SN 2005cs obtained by integrating the fluxes in the optical bands, and bolometric light curve obtained by considering also the contribution of the UV and the NIR wavelength regions (see text for more detail). Bottom: individual UV, optical, NIR light curves of SN 2005cs. Black symbols are observations reported in Tables 2–4 of this paper, red symbols are those of Tsvetkov et al. (2006) and the blue ones are from Brown et al. (2007). The dot–dashed green vertical lines mark the turn-off points of the bolometric light curve of SN 2005cs, indicating different phases in the SN evolution.

less abruptly than the light curves during the transition between the plateau and the nebular phases (see e.g. Fig. 5, bottom), and consequently the errors in the recovered magnitudes are expected to be quite small (below ∼0.1 mag).

The contribution in the UV bands was estimated making use of the photometry presented by Brown et al. (2007), and assuming negligible UV contribution during the nebular phase. The final bolometric light curve, which spans a period of about 380 d from core-collapse, is presented in Fig. 8 (top panel). The contribution of the UV bands to the luminosity during the first ∼20 d (corresponding to the peak of light in the bolometric light curve of Fig. 8) is around 60 per cent of the total luminosity, while during recombination most of the flux arises from the contribution of the optical bands (*VRI*). The NIR bands contribute mainly during the late nebular phase, when 50 per cent of the total luminosity falls in the NIR domain. In order to help the eye in evaluating the contribution of the different wavelength regions, the quasi-bolometric (*UBVRI*) light curve obtained by integrating the fluxes in the optical bands only is also shown in Fig. 8 (top panel). For completeness, most broad-band observations available in the literature, from the UV data (Brown et al. 2007) to the NIR, are displayed in Fig. 8 (bottom panel). The data presented in this paper are reported with black symbols, those from Brown et al. (2007) are shown in blue, and those of Tsvetkov et al. (2006) in red.

In Fig. 9 we show the quasi-bolometric (*UBVRI*) light curve of SN 2005cs, compared with those of some representative type IIP SNe, spanning a wide range in luminosity: SN 1999br (Hamuy 2003; Pastorello et al. 2004), SN 2004dj (Vinkó et al. 2006), SN 1999gi (Leonard et al. 2002a), SN 1999em (Hamuy et al. 2001;

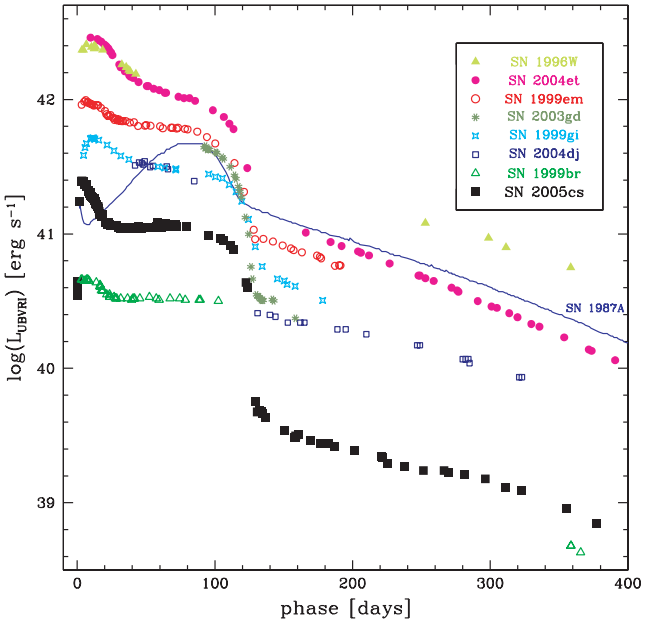

Figure 9. SN 2005cs in M51: quasi-bolometric *UBVRI* light curve of SN 2005cs compared with those of a heterogeneous sample of type IIP SNe (see text for information and references).

Leonard et al. 2002b; Elmhamdi et al. 2003a), SN 2003gd (Hendry et al. 2005), SN 2004et (Sahu et al. 2006; Kuntal et al. 2007), SN 1996W (Pastorello 2003). The plateau luminosity of SN 2005cs is lower than those of normal SNe IIP, but significantly higher than that of the extremely faint SN 1999br (Hamuy 2003; Zampieri et al. 2003; Pastorello et al. 2004). After the plateau, SN 2005cs shows a remarkably strong post-plateau decay on to the radioactive tail, deeper than that observed in any other type IIP SN in Fig. 9. As a consequence, the radioactive tail of SN 2005cs is very underluminous, close to that of SN 1999br. This is an indication of the very small mass of ^{56}Ni ejected by SN 2005cs, around 3×10^{-3} M$_{\odot}$ (obtained from a comparison with the late-time luminosity of SN 1987A), which is consistent with the amount estimated for other underluminous, ^{56}Ni-deficient SNe IIP (Pastorello et al. 2004; Spiro et al., in preparation).

4 SPECTROSCOPY

4.1 Optical spectra

The spectroscopic monitoring of SN 2005cs extended over a period of about one year. Early-time spectra (obtained during the first month after the SN discovery) were presented in Paper I. In this section we analyse the complete spectroscopic evolution of this SN, including spectra obtained during the nebular phase. Information on the spectra obtained since 2005 August (i.e. starting about one month after the discovery) is reported in Table 5, while information on earlier spectra can be found in Paper I. The full sequence of early-time spectra of SN 2005cs (phase $\leq$2 months, including also those published in Paper I) is shown in Fig. 10.

The sequence of photospheric spectra of SN 2005cs in Fig. 10 highlights the metamorphosis which occurred between the early photospheric phase (Paper I) and the middle of the recombination period. In early photospheric spectra, characterized by a very blue continuum, mostly H and He I lines are visible, with the likely presence of N II lines (see e.g. Schmidt et al. 1993; Dessart & Hillier 2005, 2006; Baron et al. 2007; Dessart et al. 2008). With time (about 1–2 weeks after explosion), the strong He I λ5876 line disappears and is replaced by Na ID ($\lambda\lambda$5890, 5896, see also the left-hand panel in Fig. 11). In this phase, also O I λ7774, Ca H&K,

Table 5. Journal of spectroscopic observations of SN 2005cs, from 2005 August to 2006 May. Information on spectra obtained before 2005 August is reported in table 2 of Paper I. The phases are computed with reference to the explosion epoch.

Date	JD +240 0000	Phase (d)	Instrumental configuration	Range (Å)	Resolution[a] (Å)
02/08/05	53585.4	36.4	L1.52 + BFOSC + gm.4	3580–8720	15
10/08/05	53593.4	44.4	TNG + DOLORES + LRB, LRR	3260–9760	14, 14
27/08/05	53610.4	61.4	TNG + DOLORES + LRB, LRR	3270–9650	12, 12
28/08/05	53611.4	62.4	TNG + NICS + gm.IJ	8700–14 540	6
11/10/05	53655.3	106.3	Ekar + AFOSC + gm.4	3670–7810	24
29/10/05	53672.7	123.7	Ekar + AFOSC + gm.4	3670–7810	24
08/11/05	53682.7	133.7	Ekar + AFOSC + gm.4	3630–7800	24
03/12/05	53708.0	159.0	HET + LRS + g2(600) + GG385	4290–7340	5
11/12/05	53715.6	166.6	Ekar + AFOSC + gm.4	3490–7820	24
22/12/05	53726.6	177.6	Ekar + AFOSC + gm.4	3490–7810	24
07/01/06	53742.9	193.9	HET + LRS + g2(600) + GG385	4290–7340	5
08/02/06	53774.7	225.7	Ekar + AFOSC + gm.4	3480–7810	24
25/03/06	53819.9	270.9	HET + LRS + g2(600) + GG385	4380–7170	5
01/04/06	53826.5	277.5	WHT + ISIS + R300B + R158R	3060–10 620	6, 9
05/04/06	53830.4	281.4	TNG + NICS + gm.IJ, HK	8670–25 750	6, 11
27/05/06	53882.6	333.6	TNG + DOLORES + LRR	5050–10 470	18

[a]As measured from the full width at half-maximum (FWHM) of the night-sky lines.
L152 = Loiano 1.52-m Cassini Telescope, INAF – Osservatorio Astronomico di Bologna, Loiano (Italy);
TNG = 3.5-m Telescopio Nazionale Galileo, Fundación Galileo Galilei – INAF, Fundación Canaria, La Palma (Canary Islands, Spain);
Ekar = 1.82-m Copernico Telescope, INAF – Osservatorio di Asiago, Mt Ekar, Asiago (Italy);
HET = 9.2-m Hobby–Eberly Telescope, McDonald Observatory, Davis Mountains (Texas, USA);
WHT = 4.2-m William Herschel Telescope, Isaac Newton Group of Telescopes, La Palma (Canary Islands, Spain).

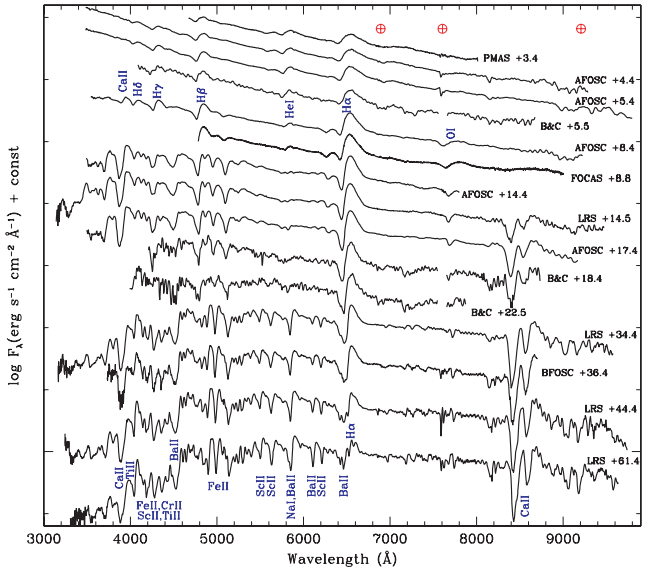

Figure 10. SN 2005cs in M51: spectral evolution during the first 2 months. The strongest spectral lines are labelled. The ⊕ symbol marks the positions of the most important telluric bands. For the codes identifying early-time spectra, see Paper I.

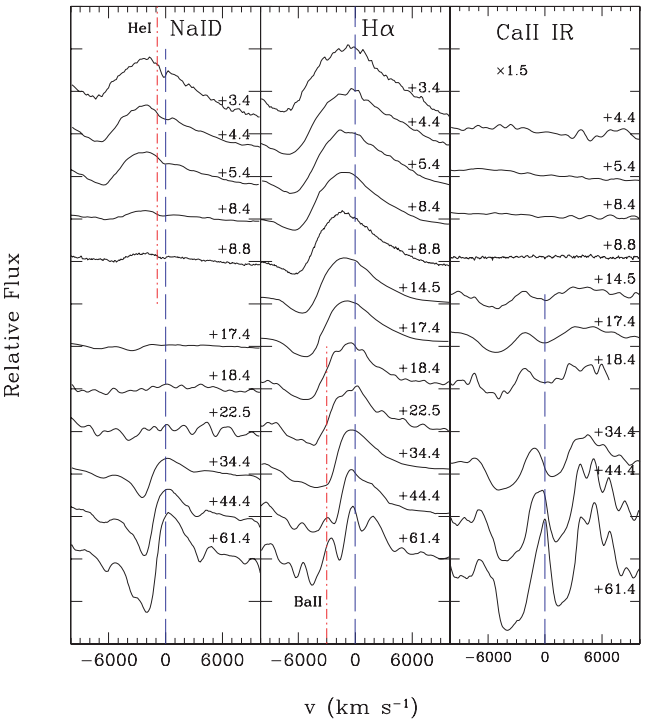

Figure 11. SN 2005cs in M51: evolution of selected spectral features during the photospheric phase. Dashed blue lines and dot–dashed red lines mark the rest wavelength positions of He I λ5876, Na ID, Ba II λ6497, Hα and Ca II λ8542.

the NIR Ca II triplet and the strongest Fe II multiplets appear. This transition phase is visualized in Fig. 11, where the most important spectral features undergo an evident transformation. In order to help the eye, the rest wavelengths of the main lines are marked.

Like in other underluminous SNe IIP (Pastorello et al. 2004), while the continuum temperature decreases due to the adiabatic

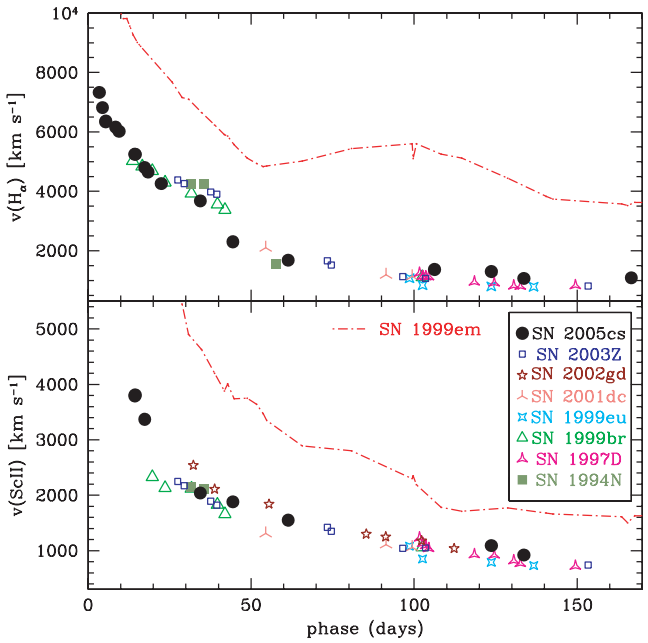

Figure 12. SN 2005cs in M51: evolution of the line velocity of Hα (top) and Sc II (bottom), and comparison with other low-luminosity SNe IIP and the normal type IIP SN 1999em.

expansion of the photosphere, the spectra become progressively redder during recombination, and a number of narrow metal lines (Fe II, Ti II, Sc II, Ba II, Cr II, Sr II, Mg II) rise to dominate the spectrum (for a detailed line identification, see Pastorello et al. 2004 and Paper I). In particular, at the red and blue wings of the Hα line, prominent lines of Ba II, Fe II and Sc II develop. In addition, Dessart et al. (2008) identify C I to be responsible for a few lines in the region between 9100 and 9600 Å. Strong line blanketing from metal lines causes a deficit of flux in the blue spectral region. Striking is the decrease of the photospheric expansion velocity during this period: the P-Cygni spectral lines become much narrower, reaching a velocity of 1000–1500 km s^{-1} at the end of the plateau (Fig. 12).

The general properties of the photospheric spectra of SN 2005cs allow us to definitely conclude that this object belongs to the well-known class of low-velocity, ^{56}Ni-poor SNe IIP (Pastorello et al. 2004). In particular, the evolution of the expansion velocities as derived from the P-Cygni minima of Hα and Sc II λ6246 nicely matches those of other events of this family (SNe 1997D, 1999br, 1999eu, 2001dc, 2002gd, 2003Z; Turatto et al. 1998; Benetti et al. 2001; Pastorello et al. 2004; Spiro et al., in preparation). The line velocities of these SNe are systematically smaller by a factor of ∼2 (see Fig. 12) with respect to the normal SN IIP 1999em (Hamuy et al. 2001; Leonard et al. 2002b; Elmhamdi et al. 2003a).

In Fig. 13 the sequence of spectra of SN 2005cs from the late photospheric phase to the nebular phase is shown. On top of the figure a spectrum of the prototypical underluminous SN 1997D (Turatto et al. 1998; Benetti et al. 2001) obtained at the end of the plateau is also included. This spectrum is shown in order to fill the gap in the spectroscopic observations of SN 2005cs during the period 62–106 d.

Fig. 14 is the analogue of Fig. 11, but in this case a few typical lines visible during the nebular phase are shown (Na ID, [O I] λλ6300, 6364, Hα and [Ca II] λλ7291, 7324). It is worth noting that the peak of Hα is always shifted towards redder wavelengths by about 700–800 km s^{-1}. This phenomenon, observed in nebular

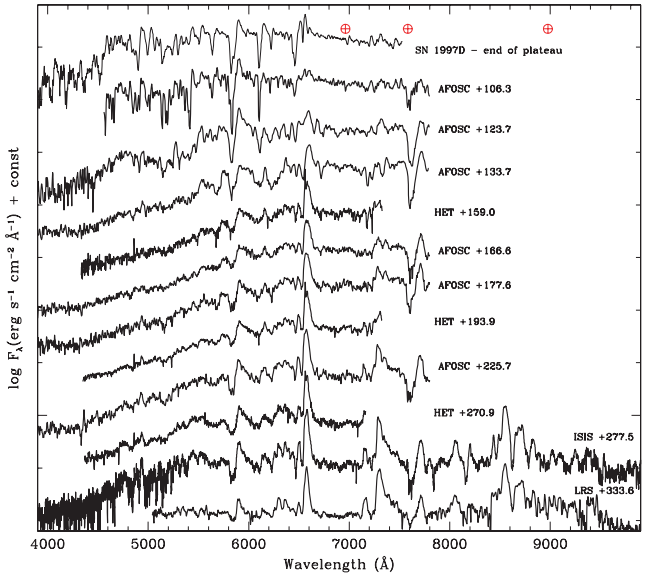

Figure 13. SN 2005cs in M51: spectroscopic transition towards the nebular phase. A spectrum of SN 1997D obtained at the end of the photospheric phase is also shown as a comparison. The position of the most important telluric bands is marked with ⊕.

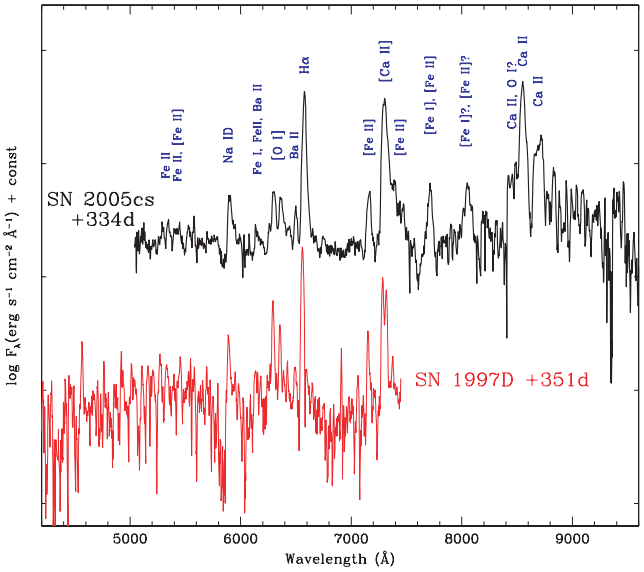

Figure 15. Comparison between nebular spectra of SN 2005cs and SN 1997D obtained about 1 yr after the explosion, with line identification. The spectrum of SN 1997D, presented in Benetti et al. (2001), has been smoothed with a boxcar size of 5 Å.

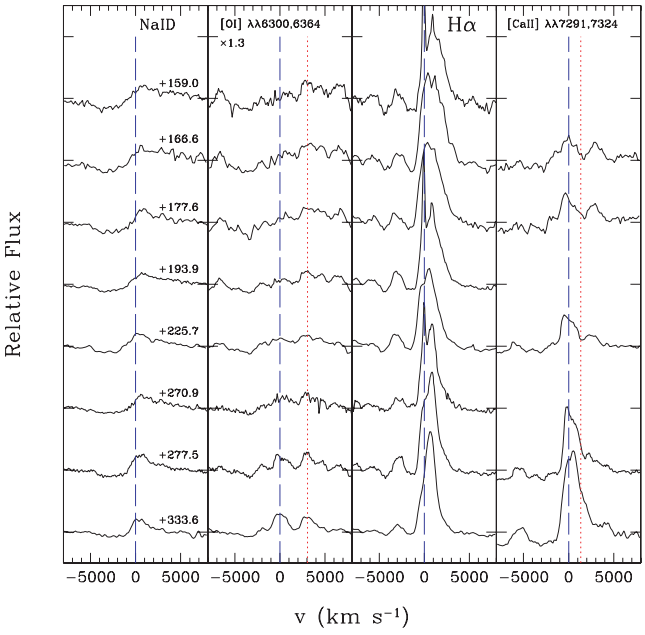

Figure 14. SN 2005cs in M51: same as Fig. 11, but during the nebular phase. Dashed blue lines and dotted red lines mark the rest wavelengths of Na ID, [O I] λλ6300, 6364, Hα and [Ca II] λλ7291, 7324. The narrow Hα component visible in the HET spectra at phases +159.0, +193.9, +270.9 is due to an improper subtraction of the background H II region.

spectra of other core-collapse SNe (e.g. SN 1987A and SN 1999em; Phillips & Williams 1991; Elmhamdi et al. 2003a) is usually interpreted as evidence of asymmetry in the ^{56}Ni distribution. Redshifted line peaks are explained with a higher hydrogen excitation due to the ejection of an excess of ^{56}Ni in the receding hemisphere. On the contrary, blueshifted peaks may be observed when most of the ^{56}Ni is ejected in the direction towards the observer (like in SN 2004dj; Chugai et al. 2005). In this context, it is worth noting that evidence of polarized radiation from early-time observations of SN 2005cs was reported by Gnedin et al. (2007), possibly an indication of asymmetric distribution of the ejected material.

The overall characteristics of the spectrum of SN 2005cs at ∼1 yr after explosion closely resemble those of other faint SNe IIP (e.g. SN 1997D, see Fig. 15), with prominent Hα, and the Na ID and NIR Ca II features still well visible. However, forbidden nebular lines are now among the strongest features visible in the spectrum. The [Ca II] λλ7291, 7324 doublet is particularly prominent, but also the [O I] λλ6300, 6364 doublet is clearly detected, though much weaker. The blue part of the spectrum of SN 2005cs (around 5300 Å) is still dominated by Fe II lines (those of the multiplet 49 are clearly visible), possibly blended with [Fe II] (multiplet 19). The Na I λλ5890, 5896 doublet still shows a residual P-Cygni profile. The weak feature at 6150 Å (according to Benetti et al. 2001) is probably due to a blend of Fe I, Fe II (multiplet 74) and Ba II (λ6142, multiplet 2) lines. The identification of Ba II in this late spectrum of SN 2005cs is confirmed by the detection of the unblended λ6497 line of the same multiplet 2. In agreement with Benetti et al. (2001), we also identify strong [Fe II] lines of the multiplet 14 (possibly with the contribution of the multiplet 30 lines) in the region of [Ca II] λλ7291, 7324. More uncertain is the identification of the strong feature at 7715 Å, which is too blueshifted to be attributed to O I λ7774. We tentatively attribute it to [Fe I] (λ7709, multiplet 1) and/or [Fe II] (λλλ7638, 7666, 7733, multiplet 30). Another strong line is visible at 8055 Å, possibly due to a blend of [Fe I] λλ8022, 8055 (multiplet 13), [Fe I] λ8087 (multiplet 24), [Fe II] λ8037 (multiplet 30) and [Fe II] λλ8010, 8012 (multiplet 46). This feature is observed in the late-time spectra of other type II SNe [e.g. in the one-year-old spectra of the SNe 1987A, 1998A, 1999em, see fig. 6 (bottom) of Pastorello et al. 2005a]. Finally, the red part of the SN 2005cs spectrum is still dominated by the prominent Ca II NIR triplet, possibly blended with O I and [Fe II] lines. Other [Fe II] lines are expected to contribute to the flux excess around 9100–9200 Å. A comprehensive identification of the nebular lines in SN 1997D can be found in Benetti et al. (2001).

According to Fransson & Chevalier (1987) and Fransson & Chevalier (1989) the ratio ($\Re$) between the luminosities of the [Ca II] λλ7291, 7324 and [O I] λλ6300, 6364 doublets is almost constant at late epochs. It is believed to be a good diagnostic for the mass of the core and, as a consequence, for the main-sequence mass of the precursor star. Objects with larger $\Re$ are expected to have smaller main-sequence masses. Elmhamdi et al. (2004, see their fig. 3) showed that most type Ib/c SNe are clustered in the region with $\Re \approx 0.3$–0.7, while for the peculiar type II SN 1987A a $\Re \approx 3$ was computed. Although Elmhamdi et al. (2004) remarked that the comparison between SNe Ib/c and SNe II may well be affected by systematic errors due to the fact that the latter have H-rich Ca II emitting regions (see also de Kool, Li & McCray 1998), the direct comparison between SN 1987A and SN 2005cs is probably reliable. The luminosities of the two doublets as measured in the last spectrum of SN 2005cs (at ∼334 d) yield $\Re \approx 4.2 \pm 0.6$, which is 40 per cent larger than that calculated for SN 1987A. This is an indication of a more modest He core and a relatively low main-sequence mass for the progenitor of SN 2005cs. This looks consistent with the relatively low progenitor masses (7–13 $M_{\odot}$) estimated by Maund et al. (2005), Li et al. (2006), Takáts & Vinkó (2006) and Eldridge et al. (2007).

4.2 Near-infrared spectra

SN 2005cs offered the rare opportunity to study the NIR spectrum of a nearby low-luminosity SN IIP. We collected two spectra of SN 2005cs, the former obtained during the photospheric phase, the latter (unfortunately with low signal-to-noise ratio) during the nebular phase (see Table 5 for more information).

In Fig. 16 the +62 days optical + NIR (*uvoir*) spectrum of SN 2005cs is compared with the *uvoir* spectrum of SN 1997D (Benetti et al. 2001) at the end of the plateau phase. The two spectra appear

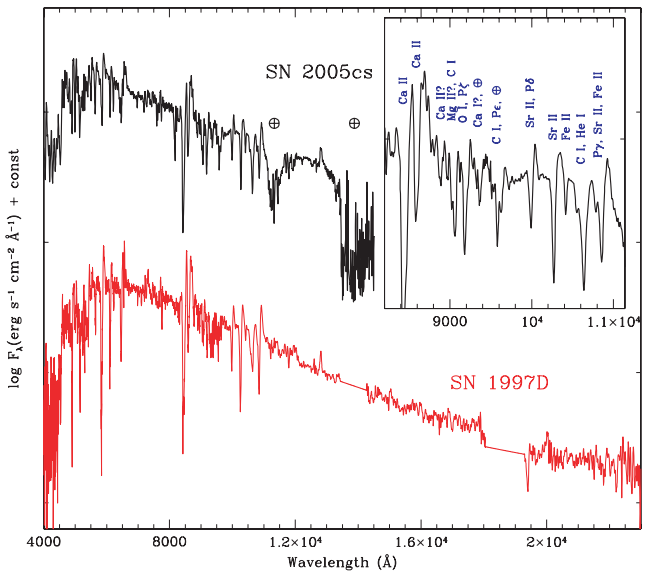

Figure 16. Comparison between *uvoir* spectra of SN 2005cs and SN 1997D obtained about 2 and 3 months, respectively, from the adopted epochs of the shock breakout. The insert (top right-hand corner) shows the line identification in the region between 8400 and 11 000 Å in the spectrum of SN 2005cs. The position of the most important near-IR telluric absorption bands is also labelled. Telluric features in the SN 2005cs spectrum have been poorly corrected because the spectrum of the telluric standard was obtained a few days after that of the SN.

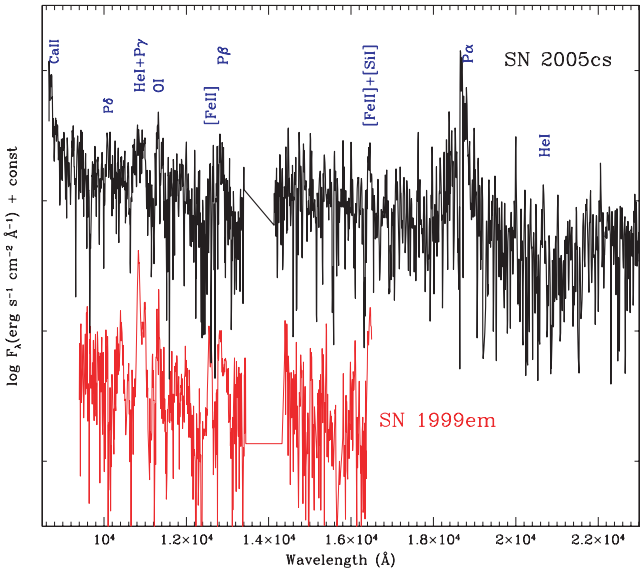

Figure 17. Comparison between the nebular NIR spectrum of SN 2005cs (phase ∼281 d) and that of SN 1999em (phase ∼444 d; Elmhamdi et al. 2003a), and tentative line identification.

to be rather similar, although that of SN 2005cs is slightly bluer owing to the one-month difference in phase. For the same reason, SN 2005cs shows slightly broader lines than SN 1997D. Nevertheless, the most important features commonly observed in type IIP SN spectra during recombination are visible in both spectra. In the insert of Fig. 16, a blow-up of the region between 8200 and 11 140 Å in the SN 2005cs spectrum is shown. The main spectral lines are identified, with the most prominent features being the NIR Ca II triplet, and blends of the H I Paschen lines with strong Sr II (multiplet 2), C I and Fe II lines. Interestingly, the classical feature at 10 850 Å is partially unblended in the spectrum of SN 2005cs owing to the narrowness of the spectral lines. It is mostly due to Pγ, Sr II λ10 915 and C I λ10 691, while the contribution of He I λ10 830 is probably less important than in other core-collapse SN types.

A second NIR spectrum of SN 2005cs was obtained at a phase of about 281 d. In Fig. 17, this spectrum is compared with that of the type IIP SN 1999em at a phase of about 15 months after explosion (Elmhamdi et al. 2003a). An attempt of line identification is made, following Bautista et al. (1995) and Pozzo et al. (2006). The strongest features visible in the spectrum are those of the Paschen series of H, and the He I λ10 830 and λ20 580 lines. A relatively strong feature at 11 310 Å is identified as the O I λ11 290 Bowen resonance line, another one at 16 445 Å as a blend of [Fe II] and [Si I]. Unfortunately, the low signal-to-noise ratio of the spectrum does not allow to clearly distinguish other spectral features.

5 CONSTRAINING THE PROGENITORS OF LOW-LUMINOSITY SNe IIP

5.1 The progenitor of SN 2005cs

The nature of the progenitors of low-luminosity SNe IIP has been extensively debated during the last decade, and only the explosions of very nearby objects could offer key information and compelling answers. This was the case with SN 2005cs, whose vicinity offered the opportunity to comprehensively analyse the spectrophotometric properties of the SN, to study in great detail the SN environment,

and to recover the progenitor star in pre-explosion archive images. The impressive quality and quantity of information collected for SN 2005cs by many groups on a wide range of wavelengths has shed light on the nature of the star generating this underluminous SN.

In Paper I and in this paper, the similarity of SN 2005cs with a number of other SN 1997D-like objects was discussed. In analogy to other events of this family, the possibility that SN 2005cs arose from the explosion of a relatively massive RSG was not ruled out (Paper I). Direct studies of the progenitor, however, seem to suggest a lower mass precursor, although mass-loss episodes in the latest phase of the evolution of the progenitor cannot be definitely excluded. This could conceivably mean that the light of the precursor star was partly extinguished by dust. However, there is evidence of low reddening towards SN 2005cs. This is key information, since the presence of dust along the line of sight would imply higher extinction, affecting the colour and luminosity estimates of the SN progenitor. As a consequence, the mass of the star would be underestimated. However, as pointed out by Eldridge et al. (2007), the non-detection of the progenitor star in the NIR pre-SN images (Maund et al. 2005; Li et al. 2006), where the effect of dust extinction on the stellar light is much weaker, is a problem for the high-reddening scenario. Therefore, the conclusions of Eldridge et al. (2007) give full support to the moderate-mass ($\leq$12 $M_\odot$) progenitor scenario proposed by Maund et al. (2005), Li et al. (2006) and Takáts & Vinkó (2006).

Baron et al. (2007), through the modelling of some early-time spectra of SN 2005cs with the PHOENIX code (Hauschildt & Baron 1999), argued that the observed spectral properties of SN 2005cs agree with an almost negligible extinction, with $E(B-V)$ being in the range 0.035–0.05. Using the non-local thermodynamic equilibrium (non-LTE) model atmosphere code CMFGEN (Hillier & Miller 1998; Dessart & Hillier 2005), Brown et al. (2007) and Dessart et al. (2008) found a similarly low extinction. Such a small extinction implies a lower intrinsic luminosity of the precursor star and a redder colour, indicating that the progenitor star was marginally less massive than reported by Maund et al. (2005) and Li et al. (2006).

As an alternative to the direct detection of the progenitor in pre-explosion images, the final stellar mass can be estimated through the modelling of the observed SN data. This approach has been applied to the cases of numerous underluminous type IIP SNe (SNe 1997D and 1999br, see e.g. Zampieri et al. 2003). The model, extensively described by Zampieri et al. (2003), makes use of a semi-analytic code that solves the energy balance equation for a spherically symmetric, homologously expanding envelope of constant density. The code computes the bolometric light curve and the evolution of line velocities and the continuum temperature at the photosphere. The physical properties of the envelope are derived by performing a simultaneous χ^2 fit of these three observables with model calculations. With the shock breakout epoch (JD = 245 3549.0 $\pm$ 0.5), distance modulus ($\mu = 29.26$) and reddening [$E(B-V) = 0.05$] adopted in this paper (see Sections 1 and 2.1), good fits are obtained with the two models shown in Fig. 18. In both models the initial radius is $R_0 = 7 \times 10^{12}$ cm (about 100 $R_\odot$) and the velocity of the expanding envelope at the onset of recombination is 1500 $\pm$ 100 km s^{-1}. However, different regions of the late time light curve of SN 2005cs are assumed to represent the true radioactive tail. Model A (dashed blue line) is obtained adopting an explosion (kinetic plus thermal) energy of $E_0 \approx 3 \times 10^{50}$ erg (0.3 foe), a ^{56}Ni mass of 2.8 ($\pm$0.2) $\times$ 10^{-3} $M_\odot$ and a relatively large total ejected mass of $M_{\rm ej} = 11.1 \pm 2.6\,M_\odot$. This model fits the bolometric light curve of SN 2005cs during the plateau and until $\sim$250 d. Model B (dot–dashed red line) results from $E_0 \approx 0.26$ foe, M(^{56}Ni) = 4.2 ($\pm$0.2) $\times$10^{-3} $M_\odot$ and $M_{\rm ej} = 9.6 \pm 1.8\,M_\odot$. The latter model has a good match with the bolometric curve at phases later than $\sim$280 d. In any case, the two models constrain the amount of ejected ^{56}Ni to be very small, about 3–4 $\times$ 10^{-3} $M_\odot$. This value is fully consistent with the ^{56}Ni mass range estimated for other low-luminosity SNe IIP (2–7 $\times$ 10^{-3} $M_\odot$; Paper I; Spiro et al., in preparation), and about one order of magnitude less than the average amount synthesized by normal type IIP SNe (Hamuy 2003; Nadyozhin 2003).

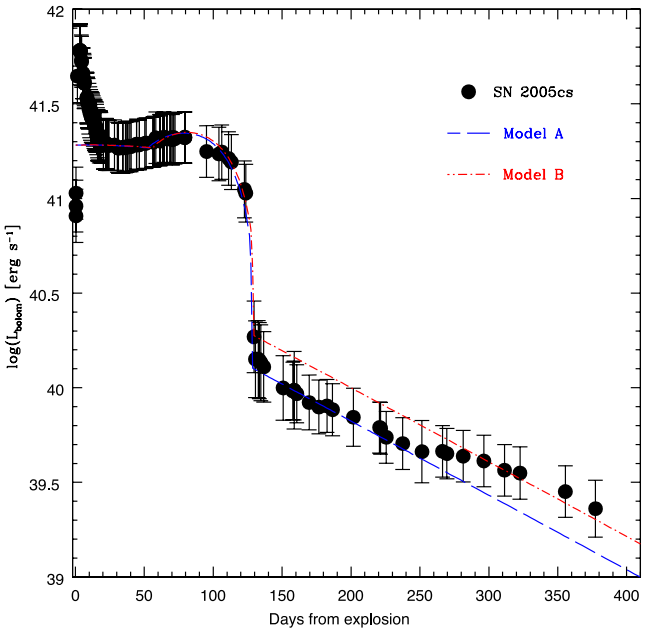

Figure 18. Comparison between the bolometric light curve of SN 2005cs (filled black points) and the two models described in the text. Model A (dashed blue line), which requires higher total ejected mass and 2.8 $\times$ 10^{-3} $M_\odot$ of ^{56}Ni, well matches the early observed radioactive tail. Model B (dot–dashed red line), instead, needs a slightly lower ejected mass and more ^{56}Ni (4.2 $\times$ 10^{-3} $M_\odot$), and fits better the late radioactive tail.

Adding the mass of a compact remnant to that of the ejected material, we may therefore constrain the final mass of the progenitor of SN 2005cs to be around 10–15 $M_\odot$ (considering the uncertainties), which is consistent with the other estimates derived through the direct detection of the progenitor star.

It is worth noting that the parameters derived here are different from those obtained by Utrobin & Chugai (2008): $R_0 = 600 \pm 140\,R_\odot$, $E_0 \approx 0.41$ foe, M(^{56}Ni) = 8.2 ($\pm$1.6) $\times$ 10^{-3} $M_\odot$ and $M_{\rm ej} = 15.9\,M_\odot$. Including the mass of the core, Utrobin & Chugai (2008) indeed obtained a larger pre-SN mass of 17.3 $\pm$ 1.0 $M_\odot$. This inconsistency can be partly explained by the significantly higher ^{56}Ni mass adopted by Utrobin & Chugai (2008), which was obtained from the overestimated radioactive tail luminosity of Tsvetkov et al. (2006) (see Section 2.3), and by different assumptions in mixing of chemical elements.

5.2 The progenitors of low-luminosity SNe IIP

There are now a number of clues indicating that SN 2005cs probably arose from a moderate-mass progenitor. However, we still need to understand whether all underluminous SNe IIP are generated by the explosion of moderate-mass stars (e.g. electron capture SNe, see Kitaura, Janka & Hillebrandt 2006; Wanajo et al. 2008), or if some of them are instead related to black hole forming massive

precursors as suggested by Zampieri et al. (1998, 2003) and Nomoto et al. (2003). The second possibility would imply that a double population of underluminous core-collapse SNe might exist, sharing similar observed properties but having different progenitors. If this is the case, which parameters may allow us to discriminate among different progenitors capable of producing faint SNe IIP?

We have to consider this possibility, since there is some degree of heterogeneity among the observables of low-luminosity SNe IIP. Contrary to what is observed in normal SNe IIP (Hamuy 2003; Pastorello 2003), the plateau magnitude in underluminous events does not seem to well correlate with the ^{56}Ni mass (see Spiro et al., in preparation). This is quite evident analysing the bolometric light curves in Fig. 3 (top) of Pastorello et al. (2005b): objects with lower average plateau luminosities are not necessarily those with deeper post-plateau luminosity drops (and, as a consequence, those having smaller ejected ^{56}Ni masses). Despite its plateau luminosity being one of the highest among the objects of this sample, SN 2005cs exhibits the largest magnitude drop (4–5 mag in the *B* band), comparable to that of SN 2002gd, and similar to those of the extremely underluminous SNe 1999br and 1999eu (Pastorello et al. 2004). Other low-luminosity SNe IIP (including e.g. SNe 1997D, 2003Z, 2001dc) drop by a more modest 2–3 mag. It is unclear, however, if this dispersion is due to intrinsic differences among the progenitors at the time of their explosion, or to a variable additional contribution from residual radiation energy, as suggested by Utrobin (2007) in the case of SN 1999em. We may speculate about the association of events showing a deep post-plateau magnitude decline with moderate-mass stars, as suggested by the magnitudes and colours of the precursor of SN 2005cs (Maund et al. 2005; Li et al. 2006) and the missing detections of the progenitors of SNe 1999br and 2006ov (van Dyk et al. 2003; Maund & Smartt 2005; Smartt et al. 2008).[2] However, while observational evidence seems to exclude very massive progenitors for faint SNe IIP similar to SN 2005cs, the issue remains open for SN 1997D and other underluminous events showing more moderate post-plateau luminosity declines. Since none of the latter has occurred in nearby galaxies, their progenitors have eluded detection in pre-explosion images so far. If the data modelling of some SNe of this group (see e.g. Zampieri et al. 2003; Utrobin, Chugai & Pastorello 2007; Zampieri 2007; Utrobin & Chugai 2008) suggests that they originate from 15–20 $M_\odot$ precursors, only the detection or a robust limit in pre-explosion images can definitely shed light on the real nature of their progenitor stars.

6 SUMMARY

New optical and near-IR data of SN 2005cs extending up to over 1-yr post-explosion are analysed together with those presented in Paper I and others from the literature. These allow us to compute for the first time a reliable bolometric light curve for a low-luminosity type IIP SN.

SN 2005cs is mildly underluminous during the plateau phase, but it has a very faint radioactive tail, suggesting that a very small amount of ^{56}Ni ($\sim 3 \times 10^{-3}\,M_\odot$) was ejected. The spectra, which are very red at the end of the H-recombination phase, show very narrow spectral lines indicative of low-velocity ejecta (about 1000–1500 km s^{-1}). All these numbers reveal the affinity of SN 2005cs to the family of underluminous, ^{56}Ni-poor, low-energy SNe IIP similar to SN 1997D.

The direct observations of the progenitor of SN 2005cs in archive images, the characteristics of the nebular spectra and the modelling of the SN data all indicate that the progenitor star was likely a moderate-mass (8–15 $M_\odot$) RSG, and not one of the massive, black hole forming stars previously proposed as the best candidates for generating 1997D-like events. However, some heterogeneity has been observed in the parameters of low-luminosity SNe IIP, and at present we cannot definitely rule out that more massive stars can similarly produce underluminous core-collapse SNe.

[2] We note that Li et al. (2007) announced the detection of the progenitor of SN 2006ov as an RSG of $15^{-3}_{+5}\,M_\odot$. However, Crockett et al. (in preparation), on the basis of a careful reanalysis of pre-SN *HST* images, questioned the correctness of the detection claimed by Li et al. (2007), since they found no star at the SN position. They estimated a mass limit for the progenitor of SN 2006ov of $\lesssim 9\,M_\odot$.

ACKNOWLEDGMENTS

SB, EC and MTB are supported by the Italian Ministry of Education via the PRIN 2006 n.2006022731-002.

This paper is partially based on observations obtained with the Hobby–Eberly Telescope, which is a joint project of the University of Texas at Austin, the Pennsylvania State University, Stanford University, Ludwig-Maximilians-Universität München and Georg-August-Universität Göttingen. This paper is also based on observations made with the Italian Telescopio Nazionale Galileo (TNG) operated on the island of La Palma by the Fundación Galileo Galilei of the INAF (Istituto Nazionale di Astrofisica), with the William Herschel and Liverpool Telescopes operated on the island of La Palma by the Isaac Newton Group at the Spanish Observatorio del Roque de los Muchachos of the Instituto de Astrofisica de Canarias, and with the AZT-24 Telescope (Campo Imperatore, Italy) operated jointly by Pulkovo observatory (St Petersburg, Russia) and INAF-Observatorio Astronomico di Roma/Collurania. The paper made also use of observations collected at the INAF-Asiago Observatory and at the Centro Astronómico Hispano Alemán (CAHA) at Calar Alto, operated jointly by the Max-Planck-Institut für Astronomie and the Instituto de Astrofísica de Andalucía (CSIC).

We acknowledge the amateur astronomers U. Bietola (Gruppo Imperiese Astrofili, http://astroimperia.altervista.org/), P. Corelli (Mandi Observatory), P. Marek (Skymaster Observatory, Variable Star Section of Czech Astronomical Society, http://www.skymaster.cz/), C. McDonnell, T. Scarmato (http://digilander.libero.it/infosis/homepage/astronomia/comet1.html), I. Uhl and the group of the Osservatorio Astronomico Geminiano Montanari (http://www.astrocavezzo.it/) for providing us their original observations.

This manuscript made use of information contained in the Bright Supernova web pages (maintained by the priceless work of D. Bishop), as part of the Rochester Academy of Sciences (http://www.RochesterAstronomy.org/snimages).

REFERENCES

Baron E., Branch D., Hauschildt P. H., 2007, ApJ, 662, 1148
Bautista M. A., Depoy D. L., Pradhan A. K., Elias J. H., Gregory B., Phillips M. M., Suntzeff N. B., 1995, AJ, 109, 729
Benetti S. et al., 2001, MNRAS, 322, 361
Brown P. J. et al., 2007, ApJ, 659, 1488
Chieffi A., Dominguez I., Höflich P., Limongi M., Straniero O., 2003, MNRAS, 345, 111
Chugai N. N., Utrobin V. P., 2000, A&A, 354, 122
Chugai N. N., Fabrika S. N., Sholukhova O. N., Goranskij V. P., Abolmasov P. K., Vlasyuk V. V., 2005, Aston. Lett., 31, 792
de Kool M., Li H., McCray R., 1998, ApJ, 503, 857

Dessart L., Hillier D. J., 2005, A&A, 437, 667
Dessart L., Hillier D. J., 2006, A&A, 447, 691
Dessart L. et al., 2008, ApJ, 675, 644
Eldridge J. J., Mattila S., Smartt S. J., 2007, MNRAS, 576, L52
Elmhamdi A. et al., 2003a, MNRAS, 338, 939
Elmhamdi A., Chugai N. N., Danziger I. J., 2003b, A&A, 404, 1077
Elmhamdi A., Danziger I. J., Cappellaro E., Della Valle M., Gouiffes C., Phillips M. M., Turatto M., 2004, A&A, 426, 963
Feldmeier J. J., Ciardullo R., Jacoby G. H., 1997, ApJ, 479, 231
Fransson C., Chevalier R. A., 1987, ApJ, 322, L15
Fransson C., Chevalier R. A., 1989, ApJ, 343, 323
Gezari S. et al., 2008, ApJ, 683, L131
Gnedin, Yu. N., Larionov V. M., Konstantinova T. S., Kopatskaya E. N., 2007, Astron. Lett., 33, 736
Hamuy M., 2003, ApJ, 582, 905
Hamuy M., Suntzeff N. B., Gonzalez R., Martin G., 1988, AJ, 95, 63
Hamuy M. et al., 2001, ApJ, 558, 615
Hauschildt P. H., Baron E., 1999, J. Comput. Appl. Math., 109, 41
Hendry M. A. et al., 2005, MNRAS, 359, 906
Hillier D. J., Miller D. L. 1998, ApJ, 496, 407
Höflich P., Straniero O., Limongi M., Dominguez I., Chieffi A., 2001, Rev. Mex. Astron. Astrofis. Ser. Conf., 10, 157
Hunt L. K., Mannucci F., Testi L., Migliorini S., Stanga R. M., Baffa C., Lisi F., Vanzi L., 1998, AJ, 115, 2594
Hunt L. K., Mannucci F., Testi L., Migliorini S., Stanga R. M., Baffa C., Lisi F., Vanzi L., 2000, AJ, 119, 985
Immler S. et al., 2007, ApJ, 664, 435
Kirshner R. P., Sonneborn G., Crenshaw D. M., Nassiopoulos G. E., 1987, ApJ, 320, 602
Kitaura F. S., Janka H.-Th., Hillebrandt W., 2006, A&A, 450, 345
Kloehr W., Muendlein R., Li W., Yamaoka H., Itagaki K., 2005, IAU Circ., 8553
Krisciunas K. et al., 2009, AJ, 137, 34
Kulkarni S. R. et al., 2007, Nat, 447, 458
Landolt A. U., 1992, AJ, 104, 340
Leonard D. C. et al., 2002a, AJ, 124, 2490
Leonard D. C. et al., 2002b, PASP, 114, 35
Li W. et al., 2003, PASP, 115, L453
Li W., Van Dyk S. D., Filippenko A. V., Cuillandre J., Jha S., Bloom J. S., Riess A. G., Livio M., 2006, ApJ, 641, L1060
Li W., Wang X., Van Dyk S. D., Cuillandre J.-C., Foley R. J., Filippenko A. V., 2007, ApJ, 661, L1013
Maund J., Smartt S. J., 2005, MNRAS, 360, 288
Maund J., Smartt S. J., Danziger I. J., 2005, MNRAS, 364, L33
Misra K., Pooley D., Chandra P., Bhattacharya D., Ray A. K., Sagar R., Lewin W. H. G., 2007, MNRAS, 381, 280
Nadyozhin D. K., 2003, MNRAS, 346, 97
Nakano S., Itagaki K., 2006, IAU Circ., 8700
Nomoto K., Maeda K., Umeda H., Ohkubo T., Deng J., Mazzali P., 2003, in van der Hucht K., Herrero A., César E., eds, IAU Symp. 212, A Massive Star Odyssey: From Main Sequence to Supernova. Astron. Soc. Pac., San Francisco, p. 395
Ofek E. O. et al., 2007, ApJ, 659, L13
Pastorello A., 2003, PhD thesis, Univ. Padova
Pastorello A. et al., 2004, MNRAS, 347, 74
Pastorello A. et al., 2005a, MNRAS, 360, 950
Pastorello A., Ramina M., Zampieri L., Navasardyan H., Salvo M., Fiaschi M., 2005b, in Marcaide J. M., Weiler K. W., eds, Proc. IAU Colloq. 192, Springer Proceedings in Physics, Vol. 99, Cosmic Explosions. Springer-Verlag, Berlin, p. 195
Pastorello A. et al., 2006, MNRAS, 370, 1752 (Paper I)
Pastorello A. et al., 2007, Nat, 449, 1
Pastorello A. et al., 2008, MNRAS, 389, 955
Phillips M. M., Williams R. E., 1991, in Woosley S. E., eds, Supernovae. The Tenth Santa Cruz Workshop in Astronomy and Astrophysics. Springer-Verlag, New York, p. 36
Pozzo M. et al., 2006, MNRAS, 368, 1169
Quimby R. M., Wheeler J. C., Höflich P., Akerlof C. W., Brown P. J., Rykoff E. S., 2007, ApJ, 666, 1093
Rau A., Kulkarni S. R., Ofek E. O., Yan L., 2007, ApJ, 659, 1536
Richmond M. W. et al., 1996, AJ, 111, 327
Sahu D. K., Anupama G. C., Srividya S., Muneer S., 2006, MNRAS, 372, 1315
Schawinski K. et al., 2008, Sci, 321, 223
Schlegel D. J., Finkbeiner D. P., Davis M., 1998, ApJ, 500, 525
Schmidt B. P. et al., 1993, AJ, 105, 2236
Smartt S. J., Eldridge J. J., Crockett R. M., Maund J. R., 2008, MNRAS, preprint (arXiv:0809.0403)
Sollerman J. et al., 2002, A&A, 386, 944
Takáts K., Vinkó J., 2006, MNRAS, 372, 1735
Tsvetkov D. Yu., Volnova A. A., Shulga A. P., Korotkiy S. A., Elmhamdi A., Danziger I. J., Ereshko M. V., 2006, A&A, 460, 769
Turatto M. et al., 1998, ApJ, 498, 129
Utrobin V. P., 2007, A&A, 461, 233
Utrobin V. P., Chugai N. N., 2008, A&A, 491, 507
Utrobin V. P., Chugai N. N., Pastorello A., 2007, A&A, 475, 973
Valenti S. et al., 2009, Nat, preprint (arXiv:0901.2074)
van Dyk S. D., Li W., Filippenko A. V., 2003, PASP, 115, 1
Vinkó J. et al., 2006, MNRAS, 369, 1780
Wanajo S., Nomoto K., Janka H.-Th., Kitaura F. S., Mueller B., 2008, ApJ, preprint (arXiv:0810.3999)
Withelock P. A. et al., 1989, MNRAS, 240, 7
Zampieri L., 2007, in AIP Conf. Proc., Vol. 924, The Multicolored Landscape of Compact Objects and Their Explosive Origins. Am. Inst. Phys., New York, p. 358
Zampieri L., Shapiro S. L., Colpi M., 1998, ApJ, 502, L149
Zampieri L., Pastorello A., Turatto M., Cappellaro E., Benetti S., Altavilla G., Mazzali P., Hamuy M., 2003, MNRAS, 338, 711

This paper has been typeset from a TEX/LATEX file prepared by the author.